Snow on Sea Ice

Robbie D.C. Mallett[a,b,c], Vishnu Nandan[b,d,e], Amy R. Macfarlane[f,g], Karley Campbell[h,b], Julienne C. Stroeve[b,c,i]

[a]*Earth Observation Group, Department of Physics and Technology, UiT The Arctic University of Norway, Hansine Hansens veg 18, Tromsø, Norway, Tromsø, 9019, Troms, Norway*
[b]*Centre For Earth Observation Science, Clayton Ridell Faculty for Environment, Earth, and Resources, University of Manitoba, Dysart Road, Winnipeg, R3T 2N2, Manitoba, Canada*
[c]*Centre for Polar Observation and Modelling, Dept. Earth Sciences, UCL, Gower Street, London, WC1E 6BS, Greater London, United Kingdom*
[d]*Cryosphere Climate Research, Group, Department of Geography, University of Calgary, 2500 University Dr NW, Calgary, T2N 1N4, Alberta, Canada*
[e]*H2O Geomatics Inc, 151 Charles St W #100, Kitchener, N2G 1H6, Ontario, Canada*
[f]*Australian Antarctic Division, 203 Channel Hwy, Kingston, Hobart, 7050, Tasmania, Australia*
[g]*WSL Institute for Snow and Avalanche Research SLF, Fluelastrasse 11, Davos Dorf, 7260, Graubunden, Switzerland*
[h]*Department of Arctic and Marine Biology, UiT The Arctic University of Norway, Hansine Hansens veg 18, Tromsø, Norway, Tromsø, 9019, Troms, Norway*
[i]*National Snow and Ice Data Center, Cooperative Institute for Research in Environmental Sciences, University of Colorado Boulder, Boulder, 80309-0449, Colorado, USA*

Abstract

The overlying snow cover on sea ice has a profound influence on what lies below. Being both highly optically reflective and thermally insulating, the snow influences the rate and timing with which the sea ice grows and melts seasonally. The shade introduced by the snow radically reduces the light intensity in and under the ice, affecting which organisms can survive there and how active they can be. As a low-density mixture of ice and air, it absorbs and scatters electromagnetic microwaves, complicating remote sensing estimates of sea ice properties. Finally, the snow's distinctive mechanical properties influence how humans live, work and travel on the ice.

Key Points:

- Snow on sea ice controls the flux of light, heat, momentum and material to the ice below.
- Its physical properties are spatiotemporally variable, being dictated by the environmental conditions such as air temperature, ice roughness, ice freeboard and wind speed.
- The snow layer complicates microwave observations of the underlying sea ice by satellites, shades photosynthesising organisms in and under the ice, and can pose additional challenges for human travel on and through the ice.

Keywords: Snow, Sea ice, Cryosphere
PACS: 9210, 9330, 9240

---

1. Introduction

Sea ice covers parts of the polar regions where the air is so cold that the surface of the ocean freezes. After forming, the sea ice almost immediately accumulates a layer of fallen snow. Snow in the sea ice system strongly affects the underlying ice by insulating the sea ice and influencing sea ice growth, delaying sea ice melt onset and consequently the sea ice seasonal cycles and its influence on sea-ice associated algal communities. Snow also influences atmospheric processes by controlling vapour fluxes and biogeochemical processes through the sea ice-snow column, contributing to sea salt aerosols through blowing snow events. The snow layer also shields the sea ice from direct observation from satellites and aircraft, leading to a host of complications in the field of sea ice remote sensing. Snow's critical role in the sea ice system led to it recently being designated an Essential Climate Variable by the World Meteorological Organisation (WMO, 2022, p 82).

This chapter begins with a description of snow on sea ice itself: its macroscopic and microscopic characteristics. Particular attention is paid to the ways in which snow on sea ice is distinct from the snow covering of mountains, glaciers, permafrost and ice sheets: this is largely through the role of *snow salinity* and snow flooding by seawater. We then turn to how the properties of snow on sea ice might be estimated at a given time using remote sensing and modelling approaches. The impacts of snow on sea ice are then described in the cases of remote sensing of sea ice thickness, in- and under-ice primary productivity and some marine mammals, and human activities in the polar oceans.

2. Key Properties and Features

2.1. Snow Albedo and Optical Depth

Snow on sea ice reflects the majority of incoming solar radiation, exhibiting a high albedo across all visible frequencies of light, leading to snow being one of the most optically reflective natural materials on Earth (Webster et al., 2018). The fraction of incoming light that is reflected can be in excess of 90% for fresh snow (Gardner and Sharp, 2010), while old or wet snow can exhibit albedo values of around 60%. This is still generally higher than the underlying sea ice, and an order of magnitude larger than a typical ocean surface (Perovich et al., 2002; Perovich and Polashenski, 2012; Light et al., 2022). The high albedo of snow therefore has a profound effect on the energy balance of the polar oceans.

Snow albedo plays a pivotal role in the polar oceans' ice-albedo feedback mechanism (Curry et al., 1995). This is a positive climate feedback, meaning that a perturbation to the system is amplified by the feedback mechanism. The ice-albedo feedback can be summarised as follows: a warming atmosphere diminishes the sea ice cover, triggering the replacement of a highly optically reflective snow surface with a relatively optically absorbant ocean surface. The new, darker ocean surface absorbs more solar energy, converting it into heat and thus warming the environment further, which further diminishes the sea ice cover.

One concept closely aligned to snow's albedo is that of optical depth. It must be stressed that the cause of the snow's high albedo is not because incoming photons of solar radiation are directly reflected by the snow surface rather than being transmitted through it. Instead, sunlight penetrates the snow surface fairly effectively, but is then strongly scattered within the upper few centimetres of the snow with weak absorption (Libois et al., 2013; Letcher et al., 2022). Because of the high ratio of scattering to absorption, the majority of photons scatter repeatedly in the upper snow volume and subsequently escape back into the air, giving snow its high albedo. The long distances travelled by photons in the upper centimetres also explains the large reductions in albedo associated with relatively low concentrations of impurities; even a few absorbing particles in the snow volume will stop a photon if the photon's path in the snow volume is long enough (Marks and King, 2014; Shi et al., 2021).

Snow's non-zero optical depth is highly relevant to the sea ice environment. Firstly, a thin covering of snow has a reduced albedo compared to a deep covering; this is because thin snow allows a fraction of photons to penetrate through to the relatively absorbing underlying sea ice (Grenfell and Perovich, 2004). This affects the radiative balance of the system, and can result in weak heating of the sea ice surface (Brandt and Warren, 1993). Secondarily, light's penetration through the snow and into the ice allows the survival of in- and under-ice primary producers (Kari et al., 2020; Castellani et al., 2022). We will return to the topic of snow's control on the light supply to primary producers in Sect. 8.2.

2.2. Thermal Conductivity

Snow is a porous mixture of ice and air, giving it a very low thermal conductivity relative to sea ice. This makes it capable of sustaining large vertical temperature gradients between the sea ice at its lower limit and the atmosphere at the top (e.g. Fig. 1). This behaviour is most noticeable in winter, when the polar atmosphere can be extremely cold, but the sea ice beneath it is kept relatively warm. Because sea ice grows thermodynamically through the transport of heat from the ocean to the atmosphere, the thermally insulating properties of snow limit thermodynamic sea ice growth when the snow surface is below freezing (Holtsmark, 1955).

The thermodynamic role of snow on sea ice mass balance in winter contrasts with the way in which it partially protects the sea ice from melting in the spring and summer (Fig. 6d of Perovich et al., 2003; Thielke et al., 2023). Several authors have therefore considered the question of whether snow's presence is a net help or hindrance to sea ice mass balance (e.g. Ledley, 1991, 1993), with Sturm and Massom (2016) couching the issue as one of "Friend or Foe?".

Snow's low thermal conductivity stems from its characteristic microstructure (Riche and Schneebeli, 2013; Macfarlane et al., 2023b): as a fine mixture of ice and air, convective, conductive and radiative transfers of heat are suppressed. Snow's low thermal conductivity also dictates its microstructural evolution (See Sect. 4). The strong thermal gradient sustained by snow on sea ice encourages the formation of *depth hoar*: large, faceted grains of snow that are weakly bonded together (Colbeck, 1982). These grains are highly

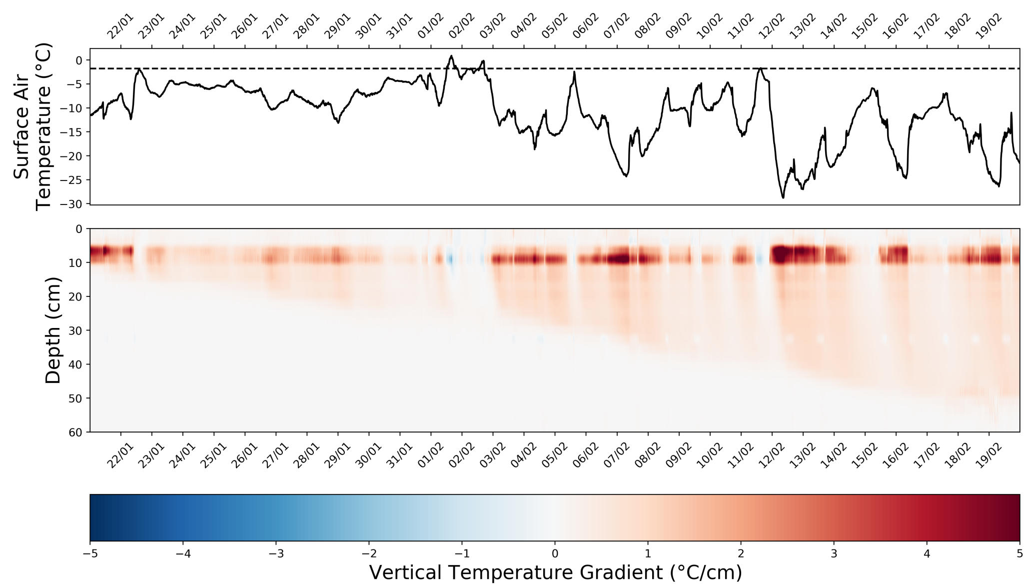

Figure 1: Thermistor-string data over a one-month period showing strong thermal insulation by a thin, ∼5cm thick snow cover over sea ice in the tank of University of Manitoba's Sea Ice Environmental Research Facility. Cold air temperatures drive a strong temperature gradient (strong red coloration) across the snow (0 - 5 cm depth) due to its low thermal conductivity. A weaker temperature gradient is present across the ice (> 10 cm depth). The ice can be seen to visibly grow over time in this data. When snow surface temperatures exceed -1.8°C, heat flows downward into the ice through the snow (blue coloration), and the snow plays a role in buffering this heat transfer.

scattering to microwaves, complicating measurements with remote sensing techniques.

2.3. Salinity

One physical property that is relatively unique to the sea ice environment is snow salinity. The salt content can be up to 20 parts per thousand (e.g. Nandan et al., 2017a). This characteristic is most common over thinner and first-year/seasonal ice types. Highest salt concentrations are generally observed above the snow/sea ice interface, with diminishing concentration with height (Fig. 2). However, snow on first-year ice can be saline throughout the pack (e.g. Drinkwater and Crocker, 1988; Barber and Nghiem, 1999). Repeated summer melt cycles over multiyear ice often cause brine drainage and flushing, which leads to negligible salinity in snow on multiyear ice and low values in the upper sea ice layers (Cox and Weeks, 1974).

Before discussing the impacts of snow salinity, it is worth considering how salt comes to exist there at all. After all, snow is fresh (i.e. not salty) when it falls from the sky, and only becomes saline afterwards. One mechanism of snowpack salinification is capillary action: this might be from the upper sea ice surface itself (on refrozen leads or at the freeze-up) or from a layer of flooded snow. As sea ice forms, some brine undergoes upward expulsion to the sea ice surface and can produce a shallow pool ($\sim$ 2 to 3 mm) of brine (Perovich and Richter-Menge, 1994). When fresh (non-salty) snow falls on this pool of brine, it can wick the brine upwards into its volume (Figure 6 of Massom et al. (2001); Figure 2 of Willatt et al. (2010)). However, it is unclear whether the supply of this brine from the newly formed sea ice surface would be sufficient to reproduce the values sometimes observed in snow pit analysis.

Another source of snow salinity is via atmospheric deposition of sea salt aerosols produced by breaking waves over the open ocean (Confer et al., 2023; Frey et al., 2020; De Leeuw et al., 2011), or in the marginal ice zones (Abbatt et al., 2012). Salt can also enter the snow through seawater flooding caused by heavy snow loading, especially on Antarctic sea ice (Massom et al., 2001; Jutras et al., 2016). The effects of flooding are discussed further in Sect. 2.4.

Another mode of snowpack salinification may be redistribution of snow that has come into contact with the ice surface during a high wind event. However, it is difficult to see how this would produce the characteristic monotonic salinity profiles. In the future, the routes through which salt arrives

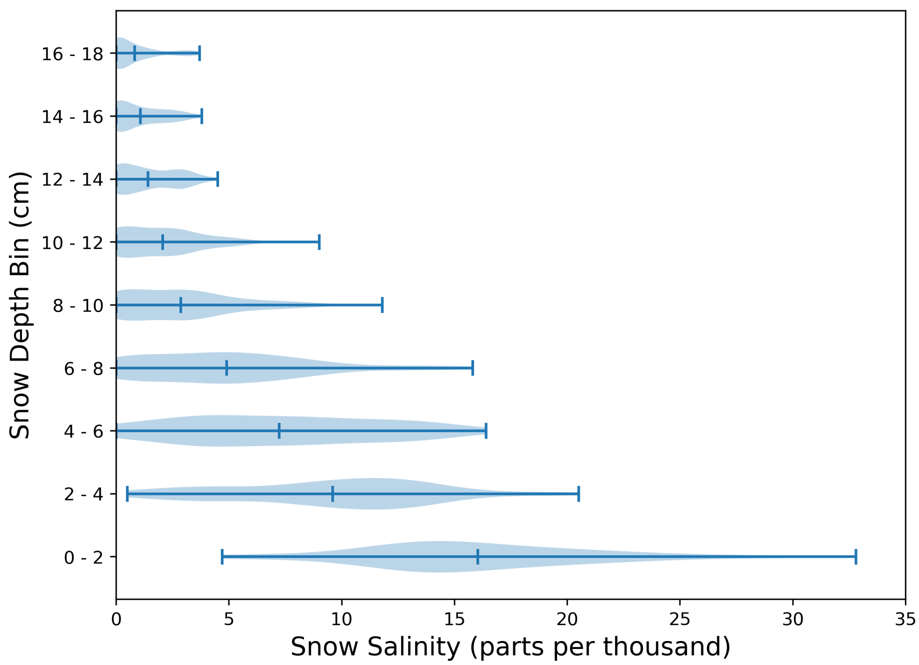

Figure 2: Vertical distribution of snow salinity in snow pits of 18 cm snow from Nandan et al. (2017a). Vertical caps mark the minimum and maximum measurements, and the mean value for the depth bin. Snow is typically most saline at the base (with the 0-2 cm layers notably exhibiting largest salinities), and least saline at the top. 0 represents the snow/sea ice interface.

in the marine snowpack could potentially be deduced by dye-tracing experiments, isotopic analysis, or controlled experiments in which flux from the sea ice is eliminated through the placement of impermeable membranes on the sea ice shortly after its formation.

Regardless of its origins, the presence of salt influences both the electromagnetic, thermodynamic, and photochemical properties of snow on sea ice (Dominé et al., 2004; Jutras et al., 2016; Nandan et al., 2020), with knock-on effects on its albedo through the timing of snowmelt onset. From optical, thermodynamic and electromagnetic perspectives, this influence is through the production of liquid water within the snow at sub-zero temperatures where it would not otherwise exist, since salt lowers the freezing point. Brine inclusions in snow have a much higher specific thermal conductivity than the ice and air that would normally make up the lattice; the presence of brine has been found to increase the snow's thermal conductivity by up to

50% (Crocker, 1984) on a thin brine-saturated snowpack on young sea ice.

Salt in snow exists in a phase equilibrium, such that brine inclusions coexist alongside the solid ice lattice of the snow. The brine volumes of both the ice and basal snow layer are smaller during winter because lower temperatures shift the phase equilibrium towards the ice phase. During melt onset, higher temperatures within the snowpack and at the snow/sea ice interface trigger an increase in brine volume at the snow basal layers (Barber and Nghiem, 1999).

As mentioned previously, salt-induced liquid water in snow also changes the snow's behaviour with regard to microwave remote sensing. Because of the water molecule's polar nature, the liquid phase is a strong absorber of microwaves across all relevant frequencies by comparison to ice. This makes it more difficult for microwaves emitted from satellite or airborne platforms to reach and return from the sea ice surface. Brine in the snowpack also makes microwaves emitted from the sea ice itself less likely to penetrate to and through the snow surface towards a radiometer.

During the winter season, snow is a significant regional source of sea salt aerosols through sublimation (Simpson et al., 2007; Yang et al., 2008) and highly-saline frost flowers growing on young sea ice surfaces (Dominé et al., 2004). Recent work (Gong et al., 2023) has highlighted the role of cloud nucleating salt aerosols from wind-blown snow in increasing the longwave radiative forcing in the Arctic.

2.4. Slush, Snow-Ice and Superimposed Ice Formation

As snow accumulates on sea ice it exerts increasing downward pressure, reducing the *sea ice freeboard*, i.e. the height to which the sea ice itself protrudes above the waterline. If snow accumulates to such an extent that the sea ice freeboard reaches zero and even becomes negative, the ice surface and the base of the snowpack can flood with seawater (Maksym and Jeffries, 2000). Due to Archimedes' law, every millimetre of accumulated snow water equivalent will reduce the ice freeboard by a corresponding millimetre (ignoring the small difference between seawater and freshwater densities). For typical values of snow and sea ice density (300 & 800 kgm^{-3} respectively), an approximate rule is that a zero freeboard will occur when the snow layer is roughly a third of the thickness of the underlying ice.

Flooding of snow (Figure 3a) due to negative freeboard is more commonly observed on Antarctic sea ice due to relatively lower ice thickness (Worby et al., 2008) and heavier snowfall. Surface melting of the sea ice itself by temperature gradient inversion (Ackley et al., 2008) may also play a role. Flooding has also been observed in some Arctic regions, for instance around Svalbard during the N-Ice field campaign (Provost et al., 2017). The increasing similarity of this region to the Southern Ocean in terms of the ratio of snow to sea ice thickness and the resulting flooding has been termed 'Antarctification' (Granskog et al., 2019). Snow flooding is mostly enabled by upward hydraulic forcing of seawater through the ice and into the snowpack (Golden et al., 1998; Massom et al., 2001), forming a slush at the base of the snowpack. Slush layers have been observed with high concentrations of sea ice algae, and can host significant fraction of sea ice chlorophyll in Antarctic sea ice (Arrigo et al., 2014; Ackley and Sullivan, 1994; Fritsen et al., 1994).

When flooded snow layers freeze, they form material known as snow-ice. After observing snow-ice thickness growing with the snow thickness over a season, Sturm et al. (1998) speculated that it forms a 'self-balancing' system which sustains near-zero freeboards on long timescales. Snow-ice can contribute significantly to the sea ice mass balance (e.g. Jeffries et al., 2001), but can also be a challenge to identify; the use of stable oxygen isotope ratios is increasingly used for this purpose (Granskog et al., 2017; Tian et al., 2020). Observations by Lange et al. (1990) showed that snow-ice can be distinguished from frazil ice by its negative δ^{18}O due to the large volumetric snow fraction. In cases where the sea ice has a variable spatial distribution of snow loading and freeboard, the presence of snow-ice has been observed to strongly control the spatial distribution of under-ice light intensity (Arndt et al., 2017).

A close but distinct relation to snow-ice is superimposed ice (Fig. 3b). Superimposed ice is formed by the melting and refreezing of snow at the ice surface (e.g. Granskog et al., 2006), or by downward percolation, pooling and refreezing of water melted at the top of the snowpack by the sun. As such, superimposed ice is mostly a form of refrozen melt-pond, with the possibility of those ponds being either exposed to the air or being contained below the snow surface ('subnivean'; Webster et al., 2022). The potential for subnivean formation is more relevant in the Southern Ocean, where melt ponds are rarely visible, but superimposed ice is often observed (Fig. 3; Haas et al., 2001; Kawamura et al., 2004; Arndt et al., 2021) By dint of its formation mechanism, superimposed ice has a considerably lower salinity than either sea ice or snow-ice, and has a distinct isotopic signature (Lange et al., 1990).

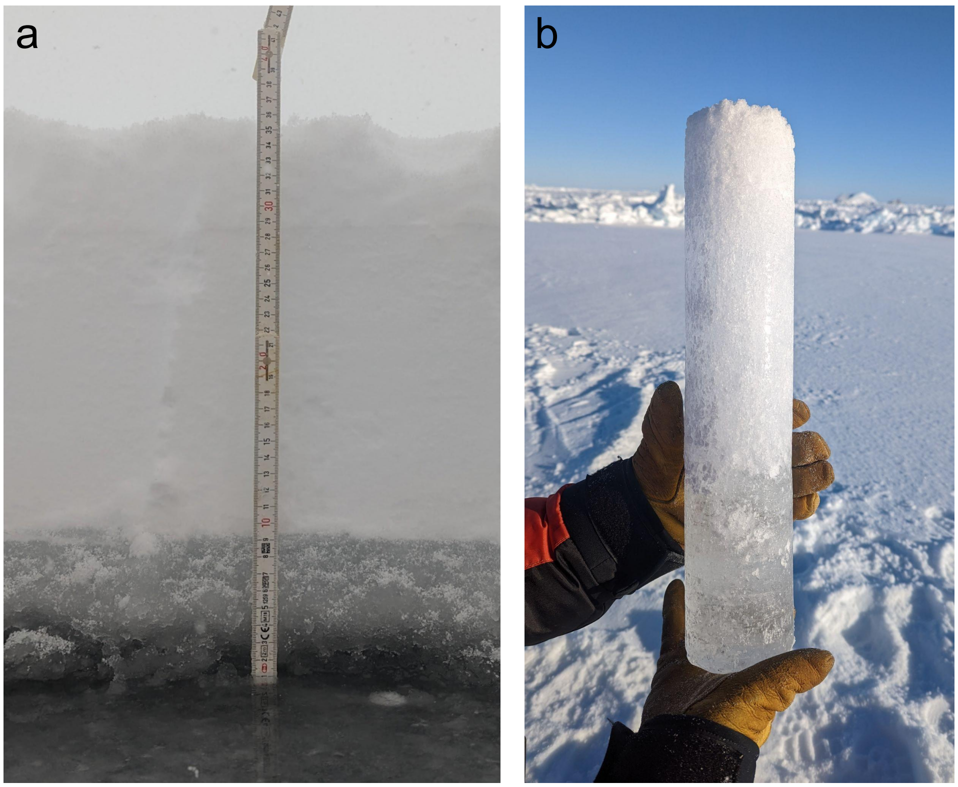

Figure 3: (a) Flooded snow on sea ice with capillary action in the Bellingshausen Sea of Antarctica. 1 cm of flooding was observed, with capillary action to a height of 8 cm above the waterline (a total of 9 cm above the ice surface). Wetted snow is visible from the grey colouring. (b) A snow core showing a 25 cm layer of superimposed ice in the Weddell Sea of Antarctica. The core transitioned from snow at the top to highly dense (900 $\mathrm{kgm^{-3}}$) ice near the bottom, which was confirmed to be fresh with salinometry.

2.5. Spatial Variability of Snow Depth Across Scales

Having so far focused on the vertical structure of the snowpack, we now turn to the horizontal variability of snow depth. This variability exists across scales, from wind-driven features on the centimetre scale known as sastrugi, to snow accumulation at pressure ridges causing snow depth variability at the meter scale, to synoptic scale variability driven by the tracking of individual weather systems, to regional variability driven by persistent water vapour pathways known as atmospheric rivers.

The sea ice environment is often a windy one, and the accumulation of homogeneous stratigraphic snow layers is uncommon in the high Arctic. These winds result in near-surface turbulence and subsequent erosion and deposition of snow such that sastrugi, dunes and other bedforms appear even when the underlying sea ice surface is level (Filhol and Sturm, 2015; Popović et al., 2020).

Wind plays a critical role in controlling the spatial and short- to long-term distribution and variability of snow depth on sea ice (Iacozza and Barber, 1999). It affects the snow residence and sintering time, influencing depositional snow dune growth and erosional processes, resulting in uneven snow depth (Savelyev et al., 2006; Filhol and Sturm, 2015; Trujillo et al., 2016).

Sea ice dynamics drive the development of ice roughness in the form of pressure ridges and rafted floes. These features cause the uneven distribution of snow depth (Fig. 4), with snow often accumulating around ridges, particularly on the downwind sides. Previous studies show the impact of wind affecting snow depth variability and redistribution on first-year sea ice over varying length scales. Using semi-variogram methods, Sturm et al. (2002) and Iacozza and Barber (1999) found 10-20 m as the short length scales controlling snow depth variability, while Moon et al. (2019) used the multi-fractal temporally weighted detrended fluctuation analysis (MF-TWDFA Koscielny-Bunde et al., 2006) and found two length scales, one at 10 m and the other between 30 m and 100 m affecting snow depth variability.

Finally, we point out that two adjacent sea ice floes may have had different lifespans, allowing them to have accumulated different amounts of snow. This introduces large-scale variability in snow depth from floe to floe (see variograms in King et al., 2015a). Inter-regional differences in snow depth also occur in both hemispheres from the different precipitation regimes (Webster et al., 2019).

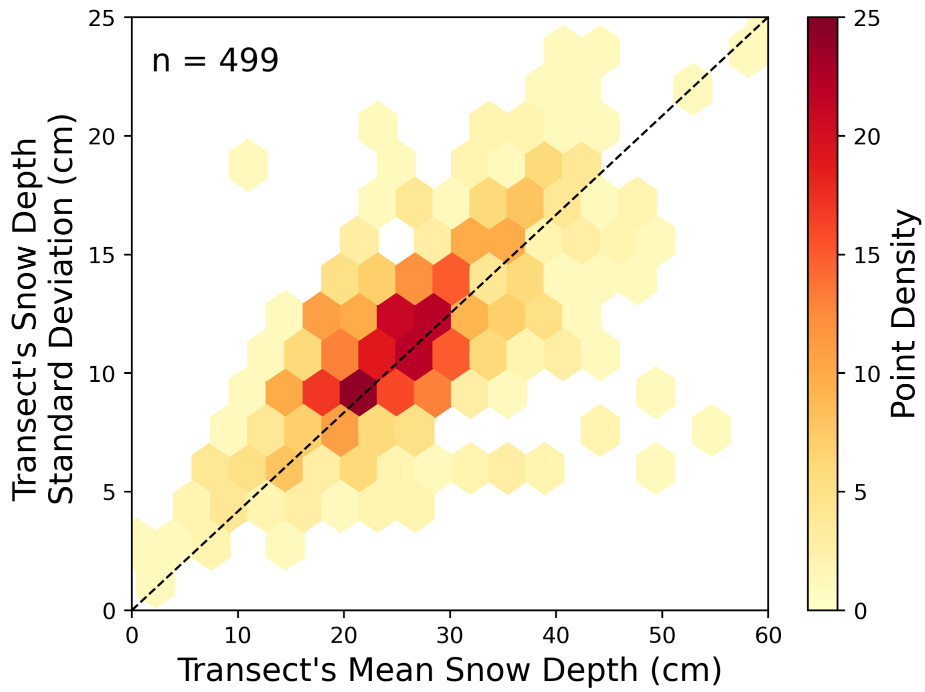

Figure 4: The relationship between the average snow depth along a 500/1000m transect, and the typical variability in snow depth along that transect. Data from Soviet North Pole drifting stations, 1954 - 1991. Most transects exhibit a snow depth between 15 - 35 cm and have a corresponding snow depth standard deviation of 8 - 13 cm. Deeper transects typically have higher variability in their snow depth. Figure following Mallett et al. (2022).

3. The Seasonal Cycle

Snow on sea ice goes through a clear seasonal cycle. A typical cycle is described here for the Arctic, with a broadly similar (but roughly antiphased) cycle occurring in the Southern Ocean.

On first-year sea ice, snow can only accumulate once the ice has formed; in the Arctic, later freeze-ups have been observed to translate into lower snow depths because accumulation is simply less possible in the high precipitation months of September and October (Webster et al., 2014; Cabaj et al., 2020). Once freeze-up has taken hold in a region, the hydrological cycle is weakened as vapour fluxes from the ocean are limited, and this reduces snowfall. In regions such as the North Atlantic sector, warm air masses can advect into the Arctic and dump large amounts of snow in a short time (e.g. Webster et al., 2019; Edel et al., 2020). However, in most regions, snow accumulates fairly steadily after freeze-up (Fig. 5).

During winter, extremely cold air temperatures lead to the characteristic two-layer slab/hoar stratigraphy described in Sect. 4, while wind-driven redistribution forms dunes and sastrugi. The diurnal temperature range in the snow and sea ice is relatively small, especially at high latitudes.

As temperatures increase during spring, transient melt events start to occur where the snow will reach 0°C, begin to melt, and then refreeze. These events are typically triggered by warm air masses advecting from outside the Arctic (see Graham et al. (2017) for an example), and can lead to noticeable changes in the snow's electromagnetic properties such as radar reflectivity and microwave emissivity (Drobot and Anderson, 2000).

The early melt season is characterised by increased solar input to the snow surface and the detection of measurable amounts of water in the snow cover. As shortwave input increases, the energy balance of the snow covered sea ice changes. The temperature gradient decreases, and diurnal temperature variability within the snow cover can be observed. Meltwater first appears sporadically between snow grains without draining (Barber et al., 1992) and up to $\sim$2% (Langlois et al., 2007), which is in the 'pendular regime' (Denoth, 1980). During early melt, the increase in snow temperature decreases the ice volume and brine salinity whilst increasing the brine volume in saline snow (Geldsetzer et al., 2009).

Continuous melt onset (Markus et al., 2009) is often identified where snow contains consistent snow moisture up to 4%, rapid snow grain metamorphism and potential formation of melt-refreeze snow/superimposed ice layers (Bar-

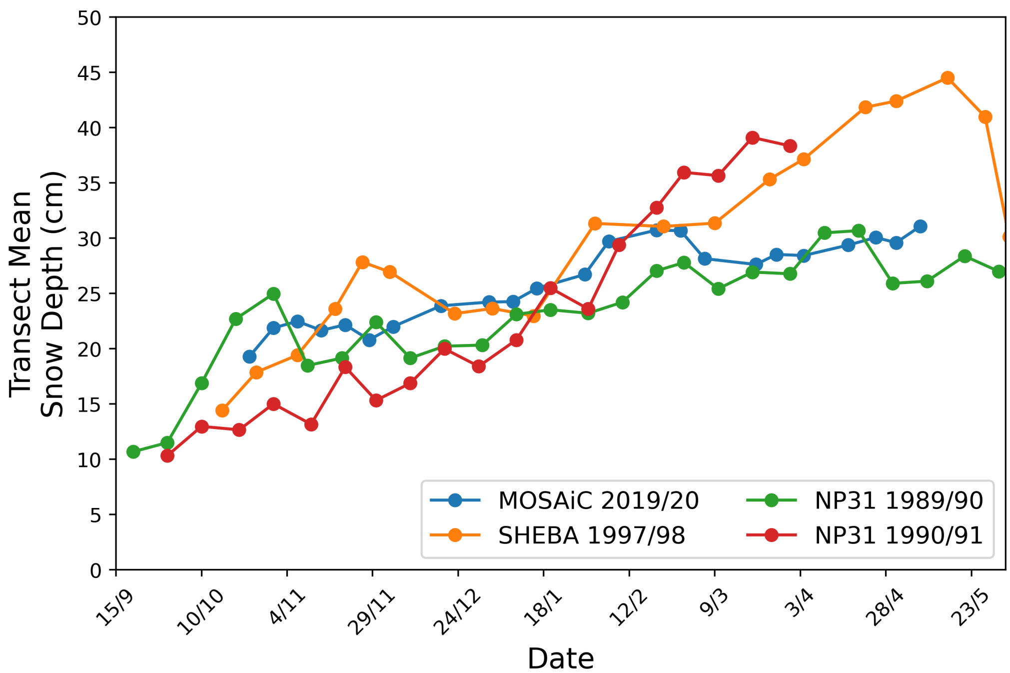

Figure 5: Winter evolution of average snow depth (September - May) in three Arctic Ocean observational campaigns (MOSAiC, SHEBA and North Pole Drifting Station 31). Snow depth increases steadily over the winter, becoming tens of centimetres thick. Settling, wind-scouring and other effects introduce reductions on short timescales. Data taken from the Northern Loop transects of MOSAiC (Itkin et al., 2021) and the Atlanta transects of SHEBA (Sturm et al., 2002). Transect protocols for North Pole drifting stations are described in Warren et al. (1999).

ber and Nghiem, 1999). Upper snow layers may exhibit melt water even at negative air temperatures due to insolation (Kane et al., 1997). During the melt onset period, snow meltwater drainage occurs due to sufficiently large snow saturation and this marks the regime change from 'pendular' to 'funicular' regime (Denoth, 1980). Snow saturation values vary as a function of grain microstructure and range between 3% (Hallikainen et al., 1987) to 14% (Denoth, 1982). By this point, the snow has lost its vertical temperature profile and is sometimes referred to as isothermal. The dynamics of melting snow involves fluid flow through a porous medium, and this remains a challenging physics problem in itself. This is in part because the grains of isothermal snow become rapidly rounded and so see significant reductions in their specific surface area (Vérin et al., 2022).

The final stage in the snow's seasonal cycle is the advanced melt phase where rapid melt of the saturated snow begins and formation of large polyaggregate snow grains occurs (Polashenski et al., 2012). Basal snow layers are supersaturated with moisture such that subnivean melt ponds may form and manifest as slush (Webster et al., 2022). This is a precursor to full melt-pond formation (Polashenski et al., 2012); ponds form in micro- to macro-scale depressions controlled by snow and ice topography (Petrich et al., 2012; Webster et al., 2015). Knolls form adjacent to these depressions, and once all the snow has melted from the sea ice surface, another snow-like structure appears, with various names throughout the literature (white ice (Malinka et al., 2016), surface granular layer (Scharien et al., 2010)), but is commonly referred to as the surface scattering layer (Smith et al., 2022; Light et al., 2022; Macfarlane et al., 2023a). Incoming shortwave radiation and preferential melt of the brine channels result in surface ablation of the sea ice and the production of a surface layer with a relatively high specific surface area and reflectivity (compared to the ice with the surface scattering layer manually removed (Smith et al., 2022)). The regeneration of this pillared layer during surface ablation of the sea ice surface ensures the sea ice albedo is consistent throughout the season (Light et al., 2022; Macfarlane et al., 2023a). This is not applicable for Antarctic sea ice, which has a persistent snow layer through summer and subnivean ponds (Webster et al., 2022).

Melt ponds amplify surface melt and warming, which in turn triggers a positive sea ice-albedo feedback which further accelerates sea ice melt (Curry et al., 1995; Stroeve et al., 2012). This important process means that sea ice models, weather and climate forecasts require high spatiotemporal observations of melt pond coverage and its evolution to function optimally (Flocco et al., 2010; Lüthje et al., 2006). Melt pond coverage varies from discrete and relatively small (<100m^2), to widespread ponded regions (> 1200 m^2) surrounded by snow/sea ice patches (Yackel et al., 2000), with pond fractions over smooth FYI between 75% (Istomina et al., 2015) and 90% (Webster et al., 2015). Areas surrounding melt ponds are characterised by thin granular snow-ice layers, highly saturated polyaggregate snow grains and melting ice surface (Scharien et al., 2010).

4. Microstructural Morphologies

While the snowpack overlying sea ice originates from falling snow, its microscopic structure (microstructure) is radically different from an assemblage of freshly precipitated snowflakes. Shortly after landing, a snowflake begins to bond to the snow around it in a process known as sintering (De Montmollin, 1982; Szabo and Schneebeli, 2007). In doing so, fallen snowflakes rapidly form a continuous lattice of ice with pore spaces of air. Lattice properties are sensitive to meteorological conditions, and they have profound effects on the bulk electromagnetic and thermodynamic properties of the snowpack. Snow microstructure over sea ice particularly reflects the strong vertical temperature gradient across the snow in winter, and the high winds to which it is typically exposed.

Historically, snow microstructure has often been characterised with reference to the grain size (e.g. Gay et al., 2002), although this is increasingly being replaced with more objectively measurable quantities such as specific surface area (e.g Matzl and Schneebeli, 2006). This is in part a recognition that snow is a bonded lattice rather than a collection of discrete elements, but also that a snowpack is made of a distribution of grain sizes (Picard et al., 2022) which are sometimes highly non-spherical (Robledano et al., 2023).

Field methods for characterising snow microstructure over sea ice have evolved rapidly over the past two decades. At the fastest and cheapest end of the spectrum lies the crystal card, or comparator card (Mallett, 2021). This tool has considerable drawbacks, which over time have driven the development of more advanced tools such as micropenetrometers (Schneebeli and Johnson, 1998) and near-infrared reflectometers (Martin and Schneebeli, 2023). Recently, micro-CT scanners have been used in the high Arctic to generate high-resolution digital models of snow microstructure (e.g. Macfarlane et al., 2023b, & Fig. 6). If a micro-CT scanner is not immediately available in the field, casting methods using diethyl-phthalate have allowed the manufacture of precise replicas of snow's interstitial pore spaces for transport and later scanning (Lombardo et al., 2021). While micropenetrometry and reflectometry offer useful proxies for snow microstructure (Kaltenborn et al., 2023), micro-CT scanning allows direct characterisation of the microstructure itself.

As mentioned in Sect. 2.2, snow on sea ice sustains significant temperature gradients between its base (adjacent to the sea ice) and its top (adjacent to the atmosphere). Furthermore, its upper surface is also often subjected to high winds, which drive a process known as *wind pumping*. These two factors are the primary drivers of snow's microstructural evolution over sea ice, and lead to a characteristic large-scale profile of microstructure in the Arctic of a depth hoar layer underlying a wind-slab (Sturm et al., 2002). In the Antarctic the situation is often more complicated due to larger snow depths and, consequently, more common flooding at the base (See Sect. 2.4). Furthermore, sea ice in the Southern Hemisphere generally exists at a lower latitude, so is exposed to a less distinct seasonal cycle and higher air temperatures.

Turning to the strong winter temperature gradient across snow on sea ice, let us first consider the typical case of a warm base (adjacent to the sea ice) and cold top (adjacent to the lower atmosphere). Key to this discussion is the concept of snow's phase equilibrium. This refers to the constant process of sublimation and condensation at the ice-air interfaces of the crystals that make up the snowpack (Dominé et al., 2003). At warmer temperatures, water molecules are more readily detached (sublimated) from the ice and thus more vapour is produced by crystals of similar shape. The vertical temperature gradient across the snow is therefore reflected by an upward vapour flux through the snowpack, and faceting of the crystals near the base, which brings them closer to phase equilibrium (Sommerfeld and LaChapelle, 1970).

This characteristic upward vapour flux has several effects on the microstructural and bulk properties of the snow. On a large scale, it hollows out lower stratigraphic layers of the snowpack and densifies upper layers, driving lower bulk densities with increasing depth over sea ice (e.g. Sect. 4.1 of King et al., 2020) This density gradient is enhanced by the effects of wind-packing, which will be addressed shortly. Microstructurally, this situation drives the development of large, coarse structures near the snowpack base known as "depth hoar" where the phase equilibrium is more active (Sturm, 1989). The threshold for the formation of the microstructures (formed through a process known as kinetic growth) is known to be around 20°C/m (Colbeck, 1982, and references therein). This faceting through kinetic growth is distinct from the

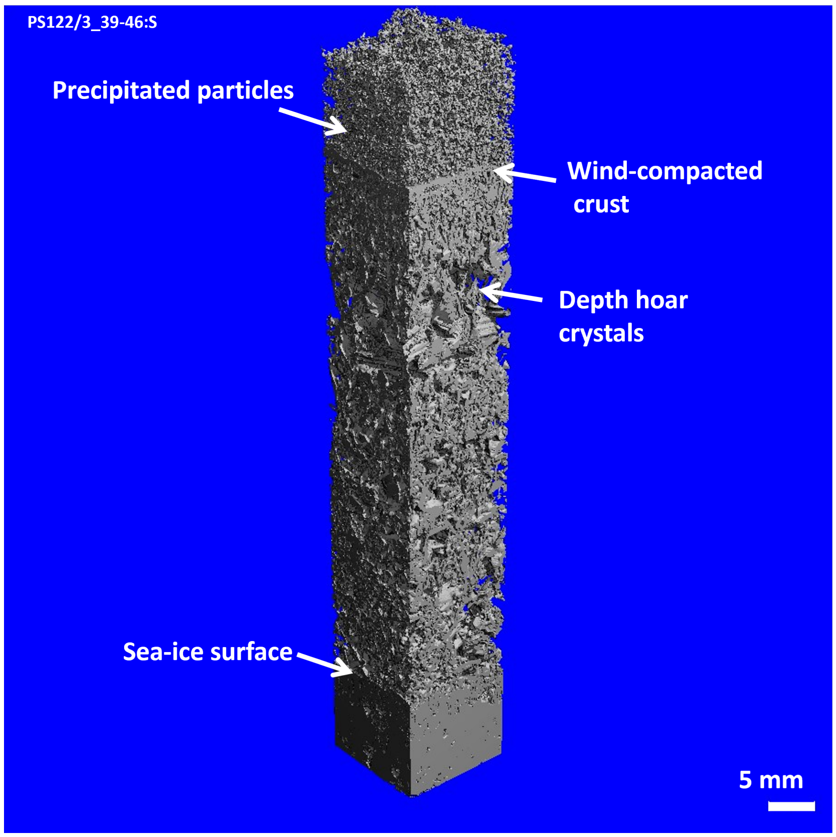

Figure 6: A micro-CT scan of a snow sample taken during the 2019/20 MOSAiC expedition (sample ID PS122/3_39-46). A sample of snow was collected in situ on sea ice and scanned onboard the research vessel RV Polarstern to obtain this 3-D reconstruction of the snow microstructure. Micro-CT snow reconstructions are used throughout snow physics research and have a variety of applications. This reconstruction is annotated with microstructural properties, but it can also be used to obtain the density, specific surface area, grain size, etc., of the snow in addition to simulations e.g. thermal conductivity.

rounding that a snow grain experiences with ageing, which occurs in the absence of any temperature gradient.

Depth hoar grains are known to be more scattering to microwaves in a remote sensing context (King et al., 2015b). To identify the role of snow microstructure (density, grain size, grain shape and arrangement) in microwave scattering, a 'microwave grain size' is required. We now know this to be proportional to the measurable optical grain size and by a factor named *polydispersity* (Picard et al., 2022).

The upper layers of snow on sea ice are frequently characterised as wind slab: this is a high-density layer resulting from wind-packing of small saltated and suspended grains, and condensed water vapour sourced both from lower levels and from wind pumping (Sommer et al., 2018). Wind slabs can develop quickly from the remobilisation and surface infiltration of wind-damaged, needle-like grains (Dominé et al., 2009) as their high specific surface area allows them to sinter rapidly and strongly (Figure 1 of Colbeck, 1991).

5. Remote Sensing of Snow on Sea Ice

Snow depth on sea ice cannot be measured in-situ with sufficient resolution in time and space to satisfy the needs of forecasters, modellers and other stakeholder communities. Such is the need for the quantity from these groups that the World Meteolorogical Organisation recently designated it an Essential Climate Variable (WMO, 2022, p. 82). The importance of this knowledge gap has also led to the development of a large number of remote sensing methods over the past forty years. The most mainstream of these will now be described, with the understanding that each has positive and negative aspects such that none can be categorically declared "the best". Consider a comparison between the satellite microwave radiometry record and that of NASA's airborne Operation Ice Bridge (OIB), which uses radar technology (Subsections 5.2 & 5.3). The former is considerably more temporally and regionally complete than the latter. However, the OIB campaigns have much better spatial resolution and accuracy along the aircraft tracks, allowing them to resolve depth variability at finer scales.

5.1. In-Situ Evaluation Methods

Before discussing the merits of individual snow depth models and retrievals, it is important to consider the means and precision with which each can be evaluated against in-situ data. This process is sometimes called validation, however this term can be misleading. Field measurements are often not directly comparable to those from remote sensing, so therefore often cannot meaningfully "validate" a remote sensing estimate in a straightforward way. Furthermore, field methods are often uncertain in themselves. As such, we encourage an evaluative approach where two uncertain quantities are compared, rather than a process where an uncertain remote sensing estimate is nominally validated against an assumed truth from the field.

In-situ characterisation of snow depth on sea ice has evolved a lot over the past 70 years. At Soviet run drifting stations (1935 - 1991), transects were performed using a ruler, and this method later shifted to the use of a graduated ski-pole (Warren et al., 1999). A significant evolution then occurred with the advent of the self-measuring probe around 1994, with a high profile deployment on sea ice during the SHEBA expedition (Sturm et al., 2002). The addition of a GPS unit allows the automatic geolocation of snow depth measurements (Sturm and Holmgren, 2018).

However, snow depth is not the only quantity of interest: snow density, specific surface area, grain size, wetness, dielectric permittivity and salinity are also key parameters to understanding remote seeing backscatter signals. Soviet stations generated a single density value by measuring the depth, and then characterising the total snow water equivalent by weighing a cylindrical core of snow. This method was superseded in sea ice field science by manual snow density measurements using density cutters of various shapes (Conger and McClung, 2009), which deliver a vertical profile of snow density. However this method is time-consuming and has driven the development of density retrievals from the Snow Micropenetrometer (Proksch et al., 2015). This is a rapid method, but has significant uncertainties which go beyond the scope of this work (e.g. King et al., 2020).

As mentioned previously, liquid water in snow also changes the snow's behaviour with regard to microwave remote sensing. Because of the polar nature of the water molecule, the liquid phase is a strong absorber of microwaves across all relevant frequencies by comparison to ice. This makes it more difficult for microwaves emitted from satellite or airborne platforms to reach and return from the sea ice surface. As a result, the wetness of a snowpack is a critical parameter often obtained using capacitance-based measurements of dielectric permittivity (e.g. Denoth and Foglar, 1985). These moisture probes have become commonplace for operational monitoring of soil moisture content in agricultural contexts, and this technology is increasingly used by sea ice teams (e.g. Geldsetzer et al., 2009).

5.2. Microwave Radiometry

Microwave radiometry provided one of the earliest avenues for characterising the snow depth over sea ice (Markus and Cavalieri, 1998). These approaches involve the measurement of natural thermal microwave radiation from the sea ice. All materials emit this type of radiation, which includes the 19 & 37 GHz (or similar) channels measured by satellite-mounted radiometers, often in different polarisations.

The most basic approach to the method relies on the principle that microwaves of higher frequencies are attenuated more strongly by the snow. A thicker snowpack therefore delivers a bigger difference between the intensity of higher frequency microwaves and lower frequency microwaves, relative to the intensities with which they are emitted by the sea ice surface. Ocean water has characteristically high brightness temperature by comparison to snow and sea ice, and therefore pollutes the signal when present in a satellite-mounted radiometer's field of view; as such, the sea ice concentration must be separately estimated and its effect controlled for as well as possible.

In addition to its sensitivity to sea ice concentration errors, snow depth retrievals using microwave radiometry have a number of other drawbacks. Firstly, the method described above using the 19 & 37 GHz channels has only been successfully deployed over first-year ice (Markus and Cavalieri, 1998). This is because snow emits its own thermal microwaves, and the emissions signature of multiyear ice is too similar to that of snow for the differential attenuation to be identified (Comiso et al., 2003; Brucker and Markus, 2013). This issue is more consequential in the Arctic, where multiyear ice makes up a much larger fraction of the total ice area (See Fig. 7). Several teams have addressed this through the use of other, lower frequency radiometers channels (Rostosky et al., 2018; Braakmann-Folgmann and Donlon, 2019; Lee et al., 2021).

Another drawback of the radiometry method of snow depth estimation is that of *saturation* for higher snow depths (see Braakmann-Folgmann and Donlon, 2019, for some discussion). The physics of microwave propagation in homogenous media such as snow results in exponential attenuation of the signal's intensity, meaning that the high-frequency (37 GHz) signal drops off initially rapidly, but then increasingly slowly until the difference between it and the low-frequency intensity does not appreciably change per unit of additional snow depth. This places an upper limit on the snow depth which

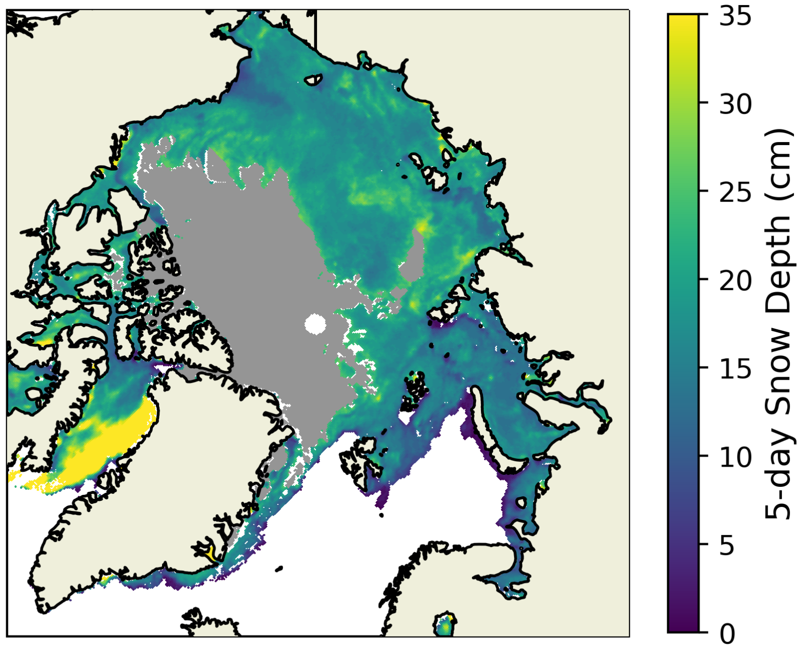

Figure 7: Snow depth retrieved over Arctic first year ice using the 37 & 19 GHz vertically polarised channels from the AMSR-E and AMSR2 radiometers. Five-day average centred on 2012/03/23, with the data set's multiyear ice mask colored in grey. Data from Meier et al. (2018).

can be retrieved with methods such as this, and this limit is typically 30 - 50 cm. This limit is particularly problematic in the Antarctic, where snow depths are typically higher. Again, the use of lower frequency channels has helped address this challenge (Shen et al., 2022).

Perhaps the most significant drawback of the passive microwave method is that it relies on the snowpack being cold and dry, such that it acts primarily as a frequency-dependent (or, for some methods, polarisation-dependent) filter on the emissions of the ice below rather than an emitter itself. This filtering behaviour is lost when liquid water emerges in the snowpack at the onset of melt, as the wet snow produces strong thermal emissions of its own. As well as being indistinguishable from the underlying ice, the wet snow also acts to absorb the microwave emissions from the ice below, further destroying the snow depth signal. While this limits the usefulness of snow depth retrievals, the behaviour has utility for the detection of snowmelt onset timing (e.g. Markus et al., 2009).

5.3. Airborne Wideband Radar Remote Sensing

Snow depth is frequently characterised using radars mounted on airborne platforms, such as the SnowRadar instrument that was used until 2019 to retrieve snow depth on sea ice for NASA's Operation Ice Bridge campaigns (Panzer et al., 2010, 2013; Kurtz and Farrell, 2011). A basic description of a radar's functionality is now given, before the application to snow depth retrievals is discussed.

At the most abstracted level, a radar instrument can be seen to emit a pulse of microwave energy and to record the power and time distribution of the reflected energy (known as backscatter). Backscatter that arrives at the detector later in time is inferred to emanate from further away. This is analogous to the sonic echo of two hands clapping near a smooth wall: if the clap's echo is heard later, the wall is understood to be further away from the clapper. Returning to the radar instrument over sea ice, an initially received pulse of reflected energy followed shortly after by a second pulse might correspond to an initial partial reflection from the snow-air interface, followed by another partial reflection from the snow-ice interface. By accounting for the reduced speed of radar-wave propagation in snow, the difference in the timing of the backscatter pulses can be transformed into an estimate of the snow depth.

SnowRadar was an "ultrawideband" radar. This refers to the wide range of frequencies used by the radar by comparison to other airborne radars (e.g.

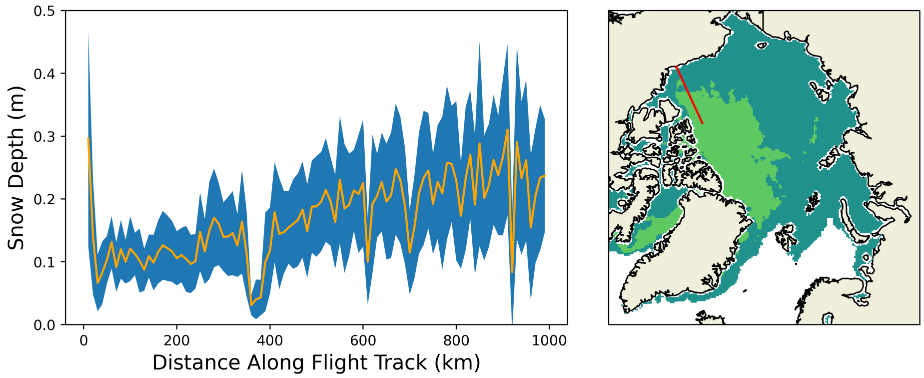

Figure 8: Left panel: Snow depth retrieved by SnowRadar on board an Operation Ice-Bridge (OIB) flight in March 2013. Orange line indicates mean snow depth of 10 km segments, blue region indicates the 1σ range of values contributing to the 10 km segment. Right panel: red line indicates flight path of the OIB flight, where "distance along flight track" in left panel is in the northbound direction. Light green indicates areas of multiyear ice on the day of the flight, dark green indicates areas of first-year ice

ASIRAS & KAREN, Hvidegaard et al., 2020). The wide frequency range allows exceptional range resolution, which in turn theoretically allows a clear identification of the ranges of the snow-air interface and snow-ice interface. However, interpreting the power timeseries produced by a radar instrument can be challenging. Spurious peaks are produced by a variety of effects, many of which are known as sidelobes. Detailing the origin and nature of radar sidelobes is beyond the scope of this chapter, but one essential impact is to make the interpretation of radar waveforms returned by snow covered sea ice non-trivial (Kwok and Maksym, 2014; Kwok and Haas, 2015). The problem and subjectivity of waveform interpretation has spurred the creation of several snow depth products from the same set of OIB radar data (Kwok et al., 2017). Part of the product of Kurtz et al. (2013) is displayed in Figure 8. These products differ among each other significantly, and as such any given product should be treated with caution. This is especially the case when the OIB data are used to "validate" other remote-sensing or modelled products.

5.4. Dual-Frequency Satellite Altimetry

The ultrawideband radar methods described above produce sufficient resolution in the radar range to theoretically allow the identification of snow-air and snow-ice interfaces in a power-range plot from one instrument (known as an echogram). However, an ultrawideband radar is large and power-hungry, making it unsuitable for satellite platforms. This is unfortunate, as airborne platforms cannot provide the spatiotemporal coverage necessary for climate change studies and many operational applications. As such, a satellite-altimeter based snow depth retrieval method is highly desirable. The general principle underpinning dual-frequency altimetry methods is that different frequencies penetrate differentially through the snowpack. This is analogous to the differential attenuation of thermal microwaves in the passive-microwave method, however it should be noted that satellite altimeters have considerably better spatial resolution than radiometers. Most methods generally assume that radar pulses in the Ku-band spectrum (12 - 18 GHz) reach and return from the snow-ice interface. By then assuming that Ka-band radar waves (26.5 - 40 GHz) return from the snow-air interface, some authors have taken the difference in Ka and Ku-band retrieved ranges to estimate snow depth (e.g. Guerreiro et al., 2016; Garnier et al., 2021). Lawrence et al. (2018) performed a calibration procedure using Operation Ice Bridge data to account for underpenetration of Ku-band radar waves and overpenetration of Ka-band radar waves, and found the calibration procedure to be fairly consequential, limiting the method to the spring season. Others have taken the difference between the Ku-band ranges and laser range retrievals to derive snow depths (Kwok et al., 2020). While it is a safer assumption to assume that lasers mostly do not penetrate the surface (relative to Ka-band radar waves), this technique suffers from the drawback of reduced temporal coverage of laser altimeters.

The Ku/Ka-band method is the operating principle for the European Space Agency's upcoming CRISTAL altimetry mission, which aims to retrieve snow depth over sea ice to within a 5 cm uncertainty (Kern et al., 2020). Establishing the snow-penetrating abilities of Ku- and Ka-band radar waves is therefore an active area of research, particularly ahead of the CRISTAL mission. Several surface-based units have been constructed and deployed on snow-covered sea ice to investigate the problem (e.g. Willatt et al., 2010; Stroeve et al., 2020b). However, these instruments struggle to measure snow on the spatial scales of a radar-altimeter's footprint, making direct comparisons challenging (De Rijke-Thomas et al., 2023). However, taken together with satellite-based (Ricker et al., 2015; Nab et al., 2023) and airborne studies (Willatt et al., 2011; King et al., 2018), a picture of inconsistent penetration of Ku-band radar is emerging. The issue of radar penetration through snow is revisited in Sect. 7 in the discussion of snow's role in complicating radar estimates of underlying sea ice thickness.

Recent work by Willatt et al. (2023) has investigated the use of two different *polarizations* of returned radar waves for detecting the snow and ice surfaces. This presents a potential new method for satellite-based snow depth retrievals; however, currently operational missions do not have the hardware required so a new instrument would need to be launched. Furthermore, it is unclear whether the cross-polarized returns that mostly indicate the range to the snow-ice interface at the surface scale would continue to do so at the satellite scale.

5.5. Imaging SAR and Scatterometry

Active microwave remote sensing using surface- and space-based microwave scatterometry and imaging synthetic aperture radar (SAR) systems has demonstrated its ability for sea ice monitoring, in large part due to its relative independence to weather (compared to optical systems) and 24-h high-resolution imaging capability (Barber et al., 1995; Yackel et al., 2000; Howell et al., 2005; Scharien et al., 2010; Mahmud et al., 2016; Nandan et al., 2017b; Scharien et al., 2017; Howell et al., 2019). The vast majority of research has been performed using Ku-, X-, C- and L-band SAR and scatterometer sensors such as QuikSCAT, ScatSAT-1, ASCAT, ERS-1/2, Envisat-ASAR, RADARSAT 1, 2 and Constellation Mission, Sentinel-1 legacy, TerraSAR-X, Cosmo SkyMed, ALOS PALSAR 1, 2 etc. However, satellite systems operate over a wide range of frequencies, spatial and temporal resolutions, polarisations and coverage over wide swath widths of 30-500 km. This intrinsically introduces sampling ambiguity due to the presence of incoherent pixels, adding uncertainty to snow geophysical interpretation and retrievals. Changes in snow geophysical properties introduce temporal decorrelation, particularly in the presence of diurnal forcing during the Spring and Autumn seasons.

Historically, our baseline understanding of microwave interactions of snow on sea ice under different geophysical and thermodynamic states has been achieved through lab- and field-based observational and theoretical studies using surface-based radar observations and microwave models, supported by quasi-coincident measurements of meteorological/snow/sea ice geophysical data (e.g. King et al., 2013; Isleifson et al., 2014; Nandan et al., 2016; Stroeve et al., 2020b; Geldsetzer et al., 2007).

Characterising active microwave backscatter from snow-covered sea ice is primarily governed by two factors: a) microwave parameters such as choice of frequency, incidence angle range and type of polarisation, and b) snow/sea ice geophysical properties, which in turn affect dielectric properties (Barber et al., 1998; Barber and Nghiem, 1999; Nandan et al., 2016). Generally, surface scattering governs at near-range incidence angles (<30°), and is caused by dielectric differences across the snow/air interface (Tjuatja et al., 1992). At larger incidence angles (>30° and <60°), snow/sea ice volume scattering is influenced by changes in snow grain size (number and density) and air/brine inclusions within the sea ice volume (Tucker et al., 2011). Generally, under cold, dry and homogenous snow/sea ice conditions, microwaves attain greater penetration through the snow volume owing to lower snow dielectric permittivity, while moisture plays a dominant role in masking penetration during the melt season (Barber et al., 1998; Barber and Nghiem, 1999). In the domain of snow on sea ice, SAR and scatterometers have been used for:

- Characterising seasonal evolution of snow thermodynamics on sea ice from Ku-band (e.g. Howell et al., 2005), C-band (Barber et al., 1998) and L-band (e.g. Mahmud et al., 2020)
- Detecting melt- and pond-onset and fractions (e.g. Barber et al., 1995; Mahmud et al., 2016; Fors et al., 2017; Scharien et al., 2017; Geldsetzer et al., 2023)
- Characterising snow/sea ice surface roughness (e.g. Fors et al., 2016; Cafarella et al., 2019; Segal et al., 2020; Huang et al., 2021)

The major disadvantage of using higher frequencies is that although microwaves provide necessary contrast between sea ice types in winter, the method fails to discriminate between ice classes during summer when snow cover is wet (Barber and Nghiem, 1999). This issue is further complicated at higher frequencies such as Ku-band where microwave backscatter is influenced by fluctuations in snow grain microstructure during melt (Howell et al., 2005). As a potential solution, Mahmud et al. (2020) and Casey et al. (2016) showed that longer wavelengths such as L-band are ideal to separate sea ice classes during the melt season compared to C-band and higher frequencies.

Quantifying snow depth on sea ice from imaging SAR and microwave scatterometers is still considered to be a challenge. Previous surface-based scatterometer and SAR studies of snow-covered FYI mentioned above have provided the physical basis towards developing an active microwave-based snow depth retrieval. Those studies show that changes in snow properties such as temperature, salinity, density and microstructure control total backscatter.

However, snow depth inversion from highly spatiotemporal snow thermodynamic changes follows complex scattering mechanisms at multiple incidence angles and polarisations at air/snow and snow/sea ice interfaces, within snow layers and volume (Barber and Nghiem, 1999; Nandan et al., 2016). Recently, Yackel et al. (2019) developed a framework to estimate relative snow depth on FYI using statistical variance in Ku- and C-band microwave backscatter from QuikSCAT and ASCAT scatterometer measurements of FYI from selected locations in the Canadian Arctic during late winters. Their study showed that a thinner snow cover shows a larger variance in daily backscatter compared to thicker snow covers. They argue that, with increase in air temperature, Ku- and C-band backscatter increases from thinner snow covers exhibiting a larger increase in snow brine volume in the basal layers (owing to stronger thermal conductivity) and an apparent increase in dielectric constant. However, it should be noted that this framework does not hold when snow depth distributions are statistically similar, suggesting similar winter backscatter variances.

6. Modelling of Snow on Sea Ice

The challenges to effective remote sensing of snow on sea ice are stark. Modelling approaches have therefore proved complementary, and come with the bonus that the effective modelling of snow cover is also critical in forecasting future polar change. Models for snow on sea ice span a range of complexities and spatio-temporal resolutions, some of which are described here.

6.1. 1D Models

It takes time for a snowpack on sea ice to be produced. For instance, a snowpack can be made up of a few individual snowfall events that generate clear stratigraphy, or it can be more a product of persistent “diamond-dusting” from the frequent but slight oversaturation of water vapour in air over sea ice (Andreas et al., 2002). The extent to which the snowpack’s stratigraphy is “event-driven” will depend on its location (e.g. Webster et al., 2019): for instance, the Barents and Kara Seas of the Arctic Ocean are exposed to storm tracks which can dump significant amounts of snow onto the sea ice at once.

One-dimensional models of snow stratigraphy and properties have a fairly long history in the terrestrial environment, which is beyond the scope of this

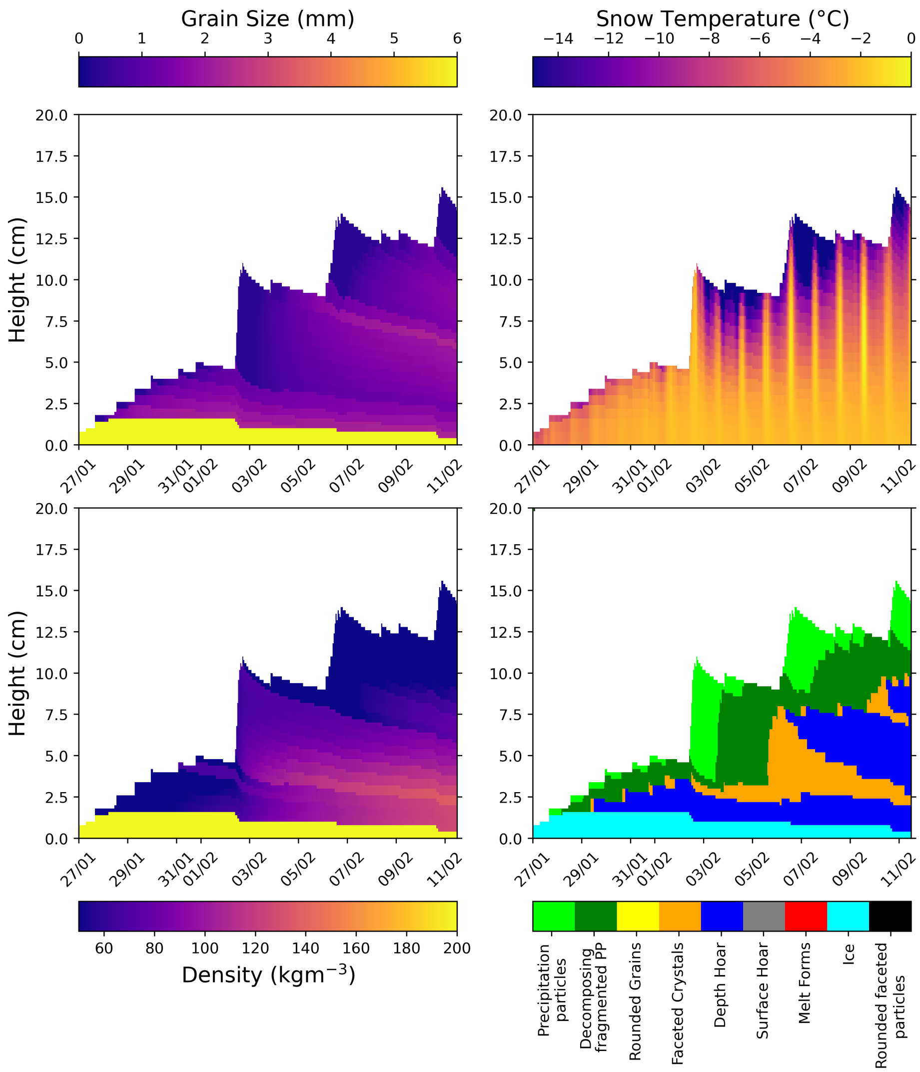

Figure 9: Sample output of the SNOWPACK 1D physical model (Wever et al., 2020) for a newly formed drifting Arctic sea ice parcel accumulating snow over a two-week period in January/February 2018. The model was driven by the ERA5 atmospheric reanalysis. Around 5 cm of snowfall is deposited on the night of the 2nd of February which causes a visible reduction in ice freeboard. Over time, the layer of deposited snow densifies, and its grains coarsen, decomposing from "precipitation particles" through to faceted crystals and depth hoar. This happens rapidly in part due to strong diurnal temperature cycling visible in the top-right panel.

chapter. In the sea ice domain, much 1D modelling is inspired by the seminal work of Maykut et al. (1971). Some high-profile models currently being applied in the sea ice domain include HIGH-TSI (Launiainen and Cheng, 1998), SNOWPACK (Wever et al., 2020), SnowModel (Liston et al., 2018), and CROCUS (Vionnet et al., 2012). The principle component of these models is to solve heat transfer and vapour flux equations at high temporal and spatial resolution relative to the snow modules in climate models. As a result, several of the models can provide physical (rather than parametrised) representations of phenomena such as snow settling, grain metamorphism, and albedo evolution. An illustrative example of SNOWPACK's output is given in Figure 9.

6.2. Spatially distributed models forced by reanalysis

One-dimensional models for snow accumulation are now regularly deployed in concert with ice motion data to produce distributed outputs of snow properties over the Arctic. However, if only the depth or snow-water-equivalent (SWE) is required, such as for altimetry applications, then an obvious first step is not to use a numerically complex model but to simply accumulate snowfall from an atmospheric reanalysis dataset. This was done by Kwok and Cunningham (2008, KC8) in order to generate sea ice thickness estimates from the ICESat laser altimetry mission. To generate the density (which is required for a sea ice thickness estimate) KC8 used a modified curve from Warren et al. (1999). KC8 used ice motion vectors to account for the effect of deeper/shallower snow being transported around the Arctic by drifting pack ice.

A more advanced method of snow modelling (which can be seen as an evolution of KC8) is the Nasa Eulerian Snow On Sea Ice Model (NESOSIM Petty et al., 2018). A critical difference between NESOSIM and KC8 is that the former contains a wind-packing scheme for snow density such that it is not climatological, and has produced data from a variety of atmospheric reanalysis datasets. NESOSIM currently forms the basis of the Goddard Space Flight Center's retrievals of sea ice thickness using the ICESat-2 laser altimeter (Petty et al., 2020).

Another step up in model complexity is SnowModel-LG (SMLG; Liston et al., 2020; Stroeve et al., 2020a). While NESOSIM is an Eulerian model (meaning that its underlying grid coordinates remain fixed), SMLG is a Lagrangian model, meaning that snow depth is modelled by individually following a number of "parcels" around the Arctic, with a regular grid of data

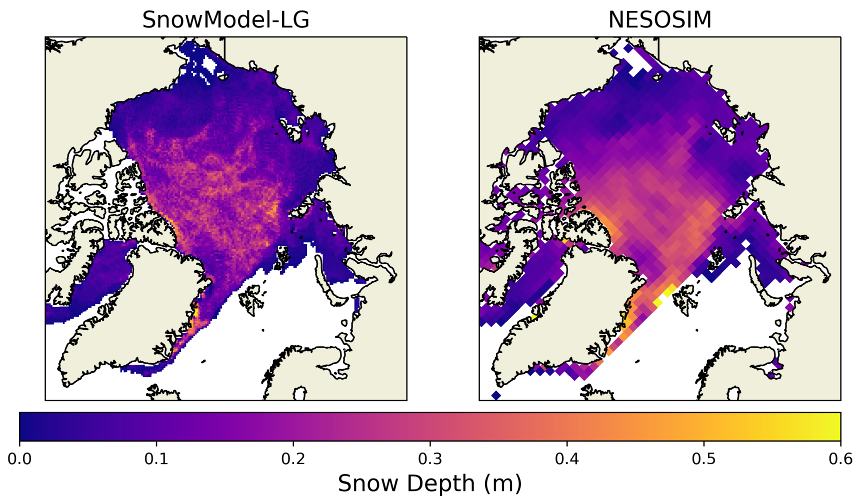

Figure 10: Snow depth on the 1st December 2015 in SnowModel-LG and NESOSIM. SnowModel-LG's Lagrangian architecture contributes to visibly finer structure in the horizontal variability of the final product.

only being produced as a final step. There are a number of advantages and disadvantages to this technique. The most obvious disadvantage is that it is computationally and arguably conceptually more complex than its Eulerian alternative. However, a Lagrangian framework allows the preservation of steeper, more realistic gradients in snow properties than would be preserved with an Eulerian approach (Fig 10). However, and perhaps crucially, the Lagrangian approach allows individual instances of a 1D model (SnowModel in this case; Liston et al., 2018) to be run for each parcel, generating a distinct spatial distribution of snow stratigraphy in Lagrangian coordinates. This is not easily possible for an Eulerian model such as NESOSIM, as it is unclear how to combine disparate snow stratigraphies when one grid cell is advecting ice into another.

It is notable that most reanalysis data sets do not include a modelled layer of snow on sea ice (Batrak and Müller, 2019; Arduini et al., 2022). As such, the snow depth cannot be extracted from reanalysis databases as meteorological data often are. The results of this omission are also noteworthy: a warm bias in the 2m temperature data is introduced, putting outputs at odds not just with in-situ and satellite-based data but also climate models, which

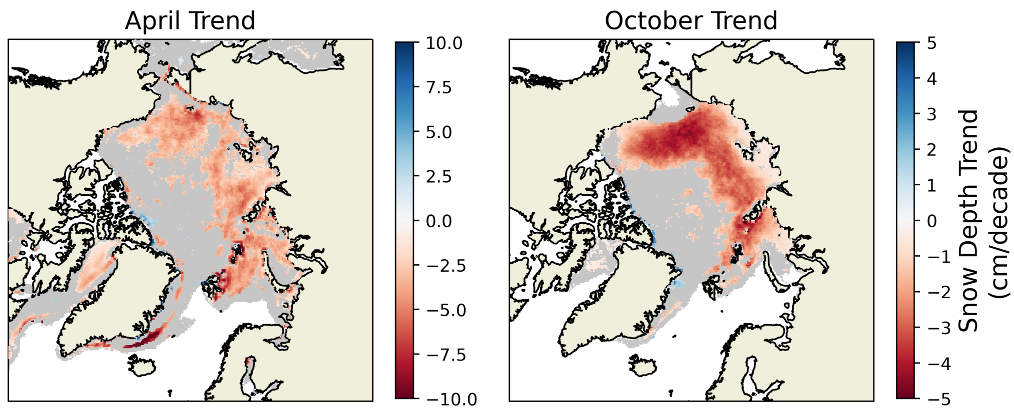

Figure 11: Trends in April and October snow depths in SnowModel-LG from 1981 - 2021. Areas where trends were calculated but found to be statistically non-significant at the 5% level are greyed out. A clear decreasing trend is seen in the Arctic's marginal seas, stemming from progressively later freeze-ups and ice-advance timings over the period.

often include snow cover on sea ice (Tian et al., 2024). This bias is relevant to physics-based models for snow on sea ice such as SnowModel which are driven by these reanalyses, and the impact of this bias has not yet been fully investigated.

With the exception of Merkouriadi et al. (2020), no spatially distributed snow model of this type has yet included either snow flooding or the thickness-dependent heat flux delivered by an underlying layer of sea ice. The impact of snow flooding from negative ice freeboard is likely much more relevant in Antarctica, a context in which the KC8 approach, NESOSIM or SMLG have not yet been run. An example of the snow depth trends produced by SnowModel-LG is shown in Figure 11.

6.3. Snow on sea ice in coupled earth systems models

Earth Systems Models (ESMs) are coupled models that incorporate atmospheric, oceanic and cryospheric dynamics among other systems. Outputs from ESMs are used to inform climate policy (for instance by the IPCC), but also in model intercomparison projects to refine projections of global change themselves. All modern ESMs participating in the sixth round of the Coupled Model Intercomparison Project (CMIP6) include sea ice modules, and these modules represent snow with variable complexity and nuance.

Snow is typically represented by a single layer (e.g. Lecomte et al. (2013)

for the NEMO-LIM model; Plante et al. (2020) for the submodule of the CICE model), and therefore cannot contain stratigraphy. This is partially justified by the conceptual challenge (discussed in Sect 6.2) of how disparate stratigraphy would be merged in an Eulerian framework, however the main justification is that of computational simplicity; it is important that the snow physics does not overly burden the speed of an ESM.

A number of other key aspects of snow physics are often omitted from earth systems models: the loss of snow to leads is one example, and the magnitude and thus importance of this potential bias remains unclear (e.g. Clemens-Sewall et al. (2023), see Liston et al. (2020) for discussion). Another example is melt-pond formation in summer: this drives significant albedo reductions in models, and where it is accounted for in ESMs the effects can be large (e.g. Flocco et al., 2012; Schröder et al., 2014; Guarino et al., 2020).

It is finally worth considering how snowfall and accumulation over sea ice is represented by these coupled models in the future. Webster et al. (2021) observed that the magnitude of the decreasing trend in snow depth is sensitive to the amount of snowfall overall in the model. It is also noteworthy that the newer generation of coupled models (CMIP6) indicate a more rapid increase in rainfall alongside intensifying snowfall (McCrystall et al., 2021). This will have significant impacts on our remote sensing of the sea ice itself (Stroeve et al., 2022). In the CESM2 model (a contributor to CMIP6), Holland and Landrum (2021) documented strong inter-hemispheric differences in the future influence of intensified snowfall on the ice mass balance: in the Southern Ocean increasing snowfall increases ice growth due to more snow-ice formation; in the Arctic, increased snow has a more thermodynamic impact, reducing mass balance by insulating the ice and stalling congelation growth.

6.4. Active and Passive Microwave Modelling

It is theoretically possible to characterise all aspects of snow on sea ice such that its thermal microwave emissions and backscattering response to an incident radar wave can be modelled to the precision required by the remote sensing community. This is particularly the case given that micro-CT analysis of the snow microstructure is increasingly available. A number of models exist such as HUT (Pulliainen and Grandeil, 1999), MEMLS (Wiesmann et al., 2000), DMRT (Tsang et al., 2000) and SMRT (Picard et al., 2018); the full expansion of these acronyms can be found in the respective, listed publications. An intercomparison of several of the models in the passive case has been carried out by Royer et al. (2017) and Saberi et al. (2020), in which the acronyms behind the model names are also given. These models are yet to be effectively validated and deployed in the active (radar) case, for several reasons which are often common to terrestrial, glacial and marine contexts. Here we will focus on only the most recent development in this field: the Snow Microwave Radiative Transfer model (SMRT; Picard et al., 2018), with particular attention paid to sea-ice-specific aspects. This narrow focus is not overly limiting, since SMRT is similar to many of the other models mentioned above, and in some cases its submodules are the same. It's noteworthy that there have been several developments to the model since its initial description paper was published in 2018.

SMRT is a one-dimensional model that, at the time of writing, can be operated in three modes: passive, active, and altimetric. It is initialised with layer-wise snow parameters such as snow temperature, microstructural parameters (such as grain size), density, salinity, and layer thickness. Recently, the Integral Equation Model has been added, such that the roughness of interfaces can be added, although this model can be numerically unstable. SMRT has the capability of simulating first-year or multiyear ice underlying the snow cover, with first-year ice consisting of brine inclusions within a saline ice matrix, and multiyear ice consisting of air-bubble inclusions in saline ice.

In passive mode, SMRT is capable of simulating brightness temperatures in the vertical and horizontal polarisations over the full range of observation angles. In active mode, SMRT acts as if a scatterometer were incident on a plane-parallel snow cover with a given small-scale roughness represented by the Integral Equation Model in terms of correlation length and RMS height. In the recently added altimetric mode (Larue et al., 2021), SMRT is capable of simulating a pulse-limited radar waveform that would be returned from plane-parallel snow. It should be noted that this does not include the synthetic-aperture mode of modern altimeters such as CryoSat-2 and Sentinel-6. It should also be considered that sea ice generally features topographic roughness (ridges, floe-scale changes in freeboard) that has a length scale well beyond what can be represented by SMRT; as such, the waveform simulated by SMRT in altimetric mode will not reflect that generated by a rough sea ice cover. This is also the case in active mode, where changes in the backscattered power to a real satellite sensor will often be a function of large-scale roughness that cannot currently be captured by SMRT. It is possible that in future, SMRT will be incorporated in active mode into a facet-based model similar to that of Landy et al. (2019).

7. Snow's Impact on Satellite-Altimeter Retrievals of Sea Ice Thickness

Sea ice thickness is a key indicator of environmental change and so it is highly desirable to monitor it from space. This is generally done with satellite-mounted altimeters of various frequencies, which generally use assumptions involving hydrostatic equilibrium to estimate the total sea ice thickness based on the freeboard of a floe and its snow loading. The uncertain role of snow on sea ice in altimetry estimates of sea ice thickness has been repeatedly highlighted by the Intergovernmental Panel on Climate Change (IPCC). The IPCC's previous Special Report on Oceans and the Cryosphere in a Changing Climate (SROCC) included snow on sea ice in a list Key Knowledge Gaps and Uncertainties, describing it as "Essentially unmeasured, limiting mass balance estimates and ice thickness retrievals" (Meredith et al., 2019, p. 275). This was reiterated by the IPCC's most recent, sixth assessment report with regard to the Cryosat-2 mission (Fox-Kemper et al., 2021, p. 1251).

7.1. Laser Altimetry

The two highest profile laser altimeters which operate over the sea ice domain are NASA's IceSat and IceSat-2 missions (Schutz et al., 2005; Abdalati et al., 2010). The way in which sea ice thickness is traditionally estimated from these satellites is described by Petty et al. (2023): essentially, a measurement is taken of the height of the snow surface above the waterline. The snow depth (obtained a priori) is then subtracted from that height, to estimate the height of the sea ice surface above the waterline. At this point, the weight of the snow and the density of the sea ice are used to estimate the thickness of the ice given the knowledge that it exists in hydrostatic equilibrium. From this description, it is clear that snow loading plays a significant role in the processing of laser data to sea ice thickness data.

One initial consideration in determining the height of the snow surface above the waterline is the potential over-penetration of the laser pulse (see Sect. 2.1 for a description of the ability for photons to penetrate the snow surface and experience multiple scattering before departing again from the snow surface). This effect is strongly affected by the wavelength of the laser, which for ICESat's surface ranging was 1064 nm (near-infrared; NIR) and for ICESat-2 is 532 (green). While over-penetration is more of a risk for NIR wavelengths of ICESat, modelling work has also indicated that over-penetration and multiple-scattering may introduce ranging biases with ICESat-2 (Smith et al., 2018). It has even been suggested that the phenomenon itself may be used to measure snow depth over Arctic sea ice (Hu et al., 2022).

"Shot-to-shot" variability in snow depth must also be considered in laser-based retrievals. To illustrate this, a conventional snow depth product (whether modelled or observed) will generally not have a spatial resolution higher than 10 km, whereas ICESat-2 data is often presented in freeboard segments less than 200m long. It can therefore be the case that a given spot-height will be lower than the mean snow depth for the grid cell in which the spot height resides. It would thus not be appropriate to naively subtract the mean snow depth from the spot height to derive a negative ice freeboard; somehow, low snow depths must be accounted for. Petty et al. (2020) contains information on this problem, summarising a number of snow redistribution functions that have been used for both the ICESat and ICESat-2 missions. This is less of a problem for radar altimeters due to their larger footprints. Nonetheless, Glissenaar et al. (2021) provides a comparison of approaches in the radar domain.

Finally, the absolute depth of the assumed snow cover introduces potential biases in laser-based sea ice thickness retrievals (e.g. Kern and Spreen, 2015). For a given ranging measurement, the assumption of additional snow depth decreases the assumed ice freeboard, and thus reduces the derived ice thickness. As such, snow products that are biased high will introduce a low bias into sea ice thickness retrievals. This is the opposite to the case for radar, where higher assumed snow depths result in thicker sea ice thickness retrievals (see below).

7.2. Radar Altimetry

Radar altimetry retrievals of sea ice thickness rely on similar concepts of hydrostatic equilibrium to the laser-based case. This is particularly the case with some processing chains that use data from the AltiKa mission, where the Ka-band radar waves are assumed by some to act like a laser ((i.e. to backscatter from the snow surface; Guerreiro et al., 2016)).

However, by far the most common frequency band for radar altimeters is the Ku-Band; this is the case for the ERS1/2, EnviSat, CryoSat-2, Sentinel-3 and HY-2B altimeters. In the Ku-band case, radar backscatter is often assumed to originate from the snow/sea-ice interface (e.g. Tilling et al., 2018), with waves having fully penetrated and returned back through the snow cover. When operating under this assumption, a given uncertainty in snow loading results in the opposite sign of uncertainty in sea ice thickness retrievals. However, compared to the laser case, the magnitudes of the induced biases are similar. It is worth noting that radar waves travel more slowly in snow than in air, and this is corrected for in all mainstream sea ice thickness products (Mallett et al., 2020).

A distinguishing characteristic of Ku-band altimetry of sea ice thickness is the contentious issue of radar penetration of the snow cover. This is a particularly active area of research ahead of the European Space Agency's planned CRISTAL altimetry mission (Kern et al., 2020), which will use both Ka and Ku-band frequencies, ostensibly assuming that they experience zero and total penetration of sea ice's snow cover respectively. Tank studies of Ku-band penetration from the 1990s (Beaven, 1995; Beaven et al., 1995) show a negligible or only a small amount of radar power returning from the snow surface, depending on the radar antenna's geometry. However, more recent field studies (Willatt et al., 2010, 2023; Jutila et al., 2022) show a much more significant return. The issue is further complicated by issues involving the footprint size of in-situ instruments relative to satellites (De Rijke-Thomas et al., 2023).

Willatt et al. (2011) examined airborne Ku-band data, finding that power again did not return consistently from the snow-ice interface. King et al. (2015a) used airborne data to statistically investigate the effective scattering height of CryoSat-2, finding that the best fit was obtained from associating the scattering height with the snow-air interface. However, it is unclear how sensitive this finding is to artificially high retrieved freeboards in the raw data set known as "Baseline-C", which has now been superseded. Studies which combine satellite data with snow information from buoys (Ricker et al., 2015) and SnowModel-LG (Nab et al., 2023) also indicate that radar does not fully penetrate on a consistent basis in the time period immediately after snowfall. On the other hand, it is clear that no consistent high bias (associated with artificially elevated scattering horizons) exists in publicly available sea ice thickness data (e.g. Figure 16 of Tilling et al., 2018). This implies that considerable further study is required before the present understanding of radar underpenetration can be incorporated into sea ice thickness retrievals.

8. Snow's Impact on Sea Ice Related Biology

8.1. Gas flux and biogeochemistry

The unique microstructure of snow, with a high specific surface area (SSA), provides surfaces for chemical reactions, enabling the transformation of gases and aerosols and facilitating reactions such as the deposition and uptake of atmospheric pollutants. Sunlight-induced photolysis reactions also occur in the Arctic snow cover (Grannas et al., 2007), affecting the abundance of important photochemical chemicals, e.g., bromine, oxides of nitrogen, nitrous acid, and formaldehyde (Hov et al., 2007), which dominate the local chemistry of the lower atmosphere and are responsible for the depletion of tropospheric ozone and gaseous mercury (Pratt et al., 2013; Baccarini et al., 2020; Benavent et al., 2022). Moreover, snow serves as a reservoir for persistent naturally occurring elements (Dominé et al., 2004; Nomura et al., 2013), organic pollutants (Lei and Wania, 2004; Meyer and Wania, 2008), and trace metals (Durnford and Dastoor, 2011), which, when released into the environment during snowmelt can accumulate in Arctic invertebrates, fish, birds and mammals, and affect the overall functioning of Arctic ecosystems (Köck et al., 1996; Wang et al., 2022).

While snow cover hinders the movement of gases between sea ice and the atmosphere, it is not an impermeable barrier. Instead, fluxes of carbon dioxide can occur through a snow cover even during winter (Nomura et al., 2018). There is large spatial and seasonal variability in such fluxes depending, in part, to the nature of the snow cover (e.g. snow structure) and its stage of melt (Tison et al., 2016, and references therein). The presence of superimposed ice (Sect. 2.4) is known to block gas diffusion (Nomura et al., 2010).

8.2. Primary Productivity

As mentioned in Sect. 2.1, sunlight is capable of penetrating through many centimetres of snow, and even greater distances in ice (Lebrun et al., 2023). Veyssière et al. (2022) measured light transmittance to the base of sea ice before and after clearing snow from the surface, and Figure 3 of their work provides an illustration of the variable degree to which snow itself controls light transmission. The penetration of light through snow covered sea ice allows photosynthetic activity of ice algae within sea ice (Leu et al., 2015), and potentially of phytoplankton beneath sea ice (Ardyna et al., 2020). A majority of ice algae live within the bottom skeletal-ice layer, and to a lesser extent within the brine network. Ice algal communities can also develop on the surface of sea ice under flooded or ponded conditions. Bottom-ice algae are understood to be shade-obligate flora, meaning that they are able to grow with near-zero quantities of light (Cota, 1985; Hancke et al., 2018). However, their adaptation to low light extremes also makes them susceptible to cell damage or even death, collectively referred to as photoinhibition, with exposure to high light levels that may be experienced with the removal or melt of snow (Campbell et al., 2015). Due to this sensitivity, a thinner snow cover does not always equate to higher biological productivity for ice algae (Michel et al., 1988; Lund-Hansen et al., 2020).

With the dependence of photosynthesis on light, the spatial variability of snow is thus tightly coupled to the distribution of ice algae (Campbell et al., 2015). This is evident across scales of variability, from the local distribution of snow drifts to inter-floe or regional differences in snow depth. The result is a described patchiness of bottom-ice algal productivity on the order of 3 m (Campbell et al., 2022) and ice algal chlorophyll *a* (Chl *a*) that represents algal biomass anywhere from five to nearly 100 meters in size (Gosselin et al., 1986; Granskog et al., 2005; Søgaard et al., 2010; Wongpan et al., 2020). One key control on the light reaching in- and under-ice algae is the impact of horizontal scatter within sea ice (Abraham et al., 2015); where even a small area of thin snow in an otherwise thickly covered landscape can produce "windows" in the snow layer, through which light can penetrate to support photosynthetic growth.

The nature of snow movement across the surface of sea ice also affects the growth of sea ice algae. Drift migration across level first-year sea ice is thought to create a more dynamic light environment than multiyear ice where snow movement is restricted by hummock features. As a result, algae within first-year ice may be more robust to sudden increases in light (Campbell et al., 2022). The more stable light environment of multiyear sea ice also supports a stronger relationship between sea ice algal growth and light transmission Lange et al. (2019).

Stroeve et al. (2021) used a satellite-based approach to show that year-to-year variability in snow depth has a significant impact on the amount of light that makes it into and through the sea ice to support these primary producers. With the dependence of sea ice algal growth on light availability, development of the bottom-ice algal bloom will first begin under the thinnest snow covers. Mundy et al. (2005) observed the greatest total Chl *a* under intermediate snow covers, with less Chl *a* under thin snow attributed to the increased thermal conductivity of the cover (e.g. Gosselin et al., 1986). The ice algal bloom will typically end first under such thin snow-covered areas due to this earlier removal from the ice following snow-ice melt, as well as photoinhibition (Campbell et al., 2015). This timing is consequential for grazing organisms at higher trophic levels like zooplankton, which have timed their reproductive cycles to benefit from the lipid-rich food resource of the ice algal bloom (Leu et al., 2011).

To study the impact of snow on the timing of ice algal blooms, known as their phenology, several studies have selectively modified snow depth. Arctic results indicate that brine drainage resulting from the temperature effects of snow addition appeared to limit abundance, but also strongly affected the species of organisms found (Gradinger et al., 1991; Grossi et al., 1987). More recent work (Campbell et al., 2015; Lund-Hansen et al., 2020) has documented a switching in the type of the relationship between snow depth and chlorophyll-a abundance over time as the snowpack evolves, where the snow first prevents light transmission then later delays ice melt. Due to the insulting effect of snow in late spring, total removal of the snow cover by severe weather event or artificial clearing can cause early termination of bottom-ice algal blooms (Campbell et al., 2015).

The onset of snowmelt plays a key role in the triggering of under-ice phytoplankton blooms (Fortier et al., 2002), largely through two mechanisms. The first is the rapid increase in transmitted PAR when the snow becomes wet (e.g. Mundy et al., 2014; Katlein et al., 2019). The second mechanism involves the creation of melt ponds, which form effective windows in the snow through which large amounts of light can be transmitted (Frey et al., 2011).

8.3. Higher Trophic levels

Literature on the impact of snow on sea ice on animals such as mammals and birds is limited. Ringed seals are often presented as the canonical example of a mammal vulnerable to changes in the sea ice's snow cover. Forming their dens in the snow cover of the sea ice (Kingsley et al., 1990), they are particularly sensitive to the projected reductions in spring snow depths in the Arctic (Hezel et al., 2012; Lindsay et al., 2021, 2023). Mahoney et al. (2021) discusses flooding of ringed seal lairs where the ratio of ice to snow thickness is poor, which may drive lair abandonment (their Sections 4.2 and 5.2).

Snow conditions on sea ice also affect polar bear populations and how they hunt seals (e.g. Hauser et al., 2023). For instance, Ferguson et al. (2001)

describes the role of hard snow in reducing foraging opportunities for bears, thus impacting habitat selection. Furthermore, bears have been observed to use snow shelters on sea ice in regions and times of sparse prey availability (Ferguson et al., 2001). Along these lines, Stirling et al. (1993) reported an absence of bears in regions in regions of landfast ice without snowdrifts. An interplay also exists between the thickness of a snow drift and the speed with which a polar bear can reach a seal pub within it, with Hammill and Smith (2011) finding that deeper snow depths resulted in less successful predation by bears. Structurally weaker (not just thinner) snow cover above seals has also been associated with increased predation by bears (Stirling and Smith, 2004; Chambellant et al., 2012).

9. Snow's Impact on Human Activities in the Polar Oceans

9.1. On-Ice hunting and travel in the Arctic

Many indigenous coastal communities in the Arctic rely on on-ice hunting and travel, making them sensitive to environmental change and natural variability in snow and ice conditions. For instance, Riewe (1991) documents the identification of seal dens by Inuit people by the formation of hoar-frost crystals on the snow above. During discussions about the role of snow in hunting, communities have identified the roughness induced by snow bedforms and the slush formed by melting and flooding to be potential hazards for snowmobile travel (Bell et al., 2015). Snow and sea ice surface roughness have a joint impact on sea ice trafficability using snowmobiles. Smoother snow provides safer travel on sea ice by snowmobile with reduced fuel consumption and minimal wear and tear on equipment. Frequent snow storms, snow hummocks, and snow drifting around rough sea ice also affect on-ice travel safety (Segal et al., 2020). Sea ice discontinuities such as pressure ridges, cracks and leads filled with snow appear deceptively trafficable for hunters to travel across, and can become a safety risk. The timing of autumn snowfall has also been identified as making seal hunting more dangerous (through stalling ice growth and promoting melt; Laidler et al., 2009). To inform community members on safe sea ice travel, community-led organisations such as the Arctic Eider Society in the Canadian Arctic regularly train local hunters and community members to take snow and sea ice observations by recording photos and videos to link indigenous knowledge and science through online platforms such as SIKU and ELOKA (Pulsifer et al., 2012; Krupnik et al., 2010).

9.2. Icebreaking Ships

The properties of snow on sea ice are also known to control the effectiveness of icebreaking ships, mostly through mechanical friction on the hull. Icebreaking hulls typically operate by sliding upwards and over sea ice until the downward force from the weight of the hull breaks the ice from above, and this is made much more difficult when the snow cover is deep or wet. This occurred in 2022 when the United Kingdom's newly built polar ship was unable to pass through fairly thin sea ice to resupply the International Thwaites Glacier Collaboration (Maritime Executive, 2022; Ralph Stevens, Personal Communication 2023). When snow is blown into the water and freezes into a sticky slush, it can also pose challenges to icebreaking ships: this has been reported in the Bay of Bothnia by hull manufacturers (Teemu Heinonen, Personal Communication 2023).

10. Summary

In this chapter we first described the various forms of snow on sea ice. From large-scale patterns of depth distribution, to the vertical structure of a layered snowpack, to microscale grain metamorphism, the marine snowpack's physical properties vary across scales in both space and time. We focused in particular on the unique aspects of snow in the sea ice environment; much of these stem from the presence of salt in the snow, and the potential for seawater flooding at its base.

We then discussed the ways in which we measure and quantify snow on sea ice through earth observation and modelling. With regard to different observational methods, tradeoffs are numerous and ubiquitous. Different data products have different strengths and weaknesses, resulting in no one product being "the best". Model outputs have similar issues, although the trades tend to be more focused around available computing power and its impact on the complexity of physics which can be represented.

Finally, we presented the impact of snow in four regards: remote sensing of sea ice thickness, primary production in and under the ice, the habitat of ringed seals and polar bears, and the use of the sea ice by humans both on foot, snowmobile, and icebreaker.

References

Abbatt, J.P., Thomas, J.L., Abrahamsson, K., Boxe, C., Granfors, A., Jones, A.E., King, M.D., Saiz-Lopez, A., Shepson, P.B., Sodeau, J., Toohey, D.W., Toubin, C., Von Glasow, R., Wren, S.N., Yang, X., 2012. Halogen activation via interactions with environmental ice and snow in the polar lower troposphere and other regions. Atmospheric Chemistry and Physics 12, 6237–6271. doi:10.5194/ACP-12-6237-2012.

Abdalati, W., Zwally, H.J., Bindschadler, R., Csatho, B., Farrell, S.L., Fricker, H.A., Harding, D., Kwok, R., Lefsky, M., Markus, T., Marshak, A., Neumann, T., Palm, S., Schutz, B., Smith, B., Spinhirne, J., Webb, C., 2010. The ICESat-2 laser altimetry mission. Proceedings of the IEEE 98, 735–751. doi:10.1109/JPROC.2009.2034765.

Abraham, C., Steiner, N., Monahan, A., Michel, C., 2015. Effects of subgrid-scale snow thickness variability on radiative transfer in sea ice. Journal of Geophysical Research: Oceans 120, 5597–5614. doi:10.1002/2015JC010741.

Ackley, S.F., Lewis, M.J., Fritsen, C.H., Xie, H., 2008. Internal melting in Antarctic sea ice: Development of "gap layers". Geophysical Research Letters 35, 11503. doi:10.1029/2008GL033644.

Ackley, S.F., Sullivan, C.W., 1994. Physical controls on the development and characteristics of Antarctic sea ice biological communities— a review and synthesis. Deep Sea Research Part I: Oceanographic Research Papers 41, 1583–1604. doi:10.1016/0967-0637(94)90062-0.

Andreas, E.L., Guest, P.S., Persson, P.O.G., Fairall, C.W., Horst, T.W., Moritz, R.E., Semmer, S.R., 2002. Near-surface water vapor over polar sea ice is always near ice saturation. Journal of Geophysical Research C: Oceans 107, 1–15. doi:10.1029/2000jc000411.

Arduini, G., Keeley, S., Day, J.J., Sandu, I., Zampieri, L., Balsamo, G., 2022. On the Importance of Representing Snow Over Sea-Ice for Simulating the Arctic Boundary Layer. Journal of Advances in Modeling Earth Systems 14, e2021MS002777. doi:10.1029/2021MS002777.

Ardyna, M., Mundy, C.J., Mayot, N., Matthes, L.C., Oziel, L., Horvat, C., Leu, E., Assmy, P., Hill, V., Matrai, P.A., Gale, M., Melnikov, I.A., Arrigo, K.R., 2020. Under-Ice Phytoplankton Blooms: Shedding Light on the "Invisible" Part of Arctic Primary Production. Frontiers in Marine Science 7, 985. doi:10.3389/FMARS.2020.608032/BIBTEX.

Arndt, S., Haas, C., Meyer, H., Peeken, I., Krumpen, T., 2021. Recent observations of superimposed ice and snow ice on sea ice in the northwestern Weddell Sea. Cryosphere 15, 4165–4178. doi:10.5194/TC-15-4165-2021.

Arndt, S., Meiners, K.M., Ricker, R., Krumpen, T., Katlein, C., Nicolaus, M., 2017. Influence of snow depth and surface flooding on light transmission through Antarctic pack ice. Journal of Geophysical Research: Oceans 122, 2108–2119. doi:10.1002/2016JC012325.

Arrigo, K.R., Brown, Z.W., Mills, M.M., 2014. Sea ice algal biomass and physiology in the Amundsen Sea, Antarctica. Elementa 2, 28. doi:10.12952/JOURNAL.ELEMENTA.000028/112943.

Baccarini, A., Karlsson, L., Dommen, J., Duplessis, P., Vüllers, J., Brooks, I.M., Saiz-Lopez, A., Salter, M., Tjernström, M., Baltensperger, U., Zieger, P., Schmale, J., 2020. Frequent new particle formation over the high Arctic pack ice by enhanced iodine emissions. Nature Communications 2020 11:1 11, 1–11. doi:10.1038/s41467-020-18551-0.

Barber, D.G., Fung, A.K., Grenfell, T., Nghiem, S., Onstott, R., Lytle, V., Perovich, D., Gow, A., 1998. The role of snow on microwave emission and scattering over first-year sea ice. IEEE Transactions on Geoscience and Remote Sensing 36, 1750–1763. doi:10.1109/36.718643.

Barber, D.G., LeDrew, E.F., Flett, D.G., Shokr, M., Falkingham, J., 1992. Seasonal and Diurnal Variations in SAR Signatures of Landfast Sea Ice. IEEE Transactions on Geoscience and Remote Sensing 30, 638–642. doi:10.1109/36.142948.

Barber, D.G., Nghiem, S.V., 1999. The role of snow on the thermal dependence of microwave backscatter over sea ice. Journal of Geophysical Research: Oceans 104, 25789–25803. doi:10.1029/1999JC900181.

Barber, D.G., Reddan, S.P., Ledrew, E.F., 1995. Statistical characterization of the geophysical and electrical properties of snow on Landfast first-year sea ice. Journal of Geophysical Research: Oceans 100, 2673–2686. doi:10.1029/94JC02200.

Batrak, Y., Müller, M., 2019. On the warm bias in atmospheric reanalyses induced by the missing snow over Arctic sea-ice. Nature Communications 2019 10:1 10, 1–8. doi:10.1038/s41467-019-11975-3.

Beaven, S., 1995. Sea ice radar backscatter modeling, measurements, and the fusion of active and passive microwave data. Ph.D. thesis. Radar Systems and Remote Sensing Laboratory.

Beaven, S.G., Lockhart, G.L., Gogineni, S.P., Hosseinmostafa, A.R., Jezek, K., Gow, A.J., Perovich, D.K., Fung, A.K., Tjuatja, S., 1995. Laboratory measurements of radar backscatter from bare and snow-covered saline ice sheets. International Journal of Remote Sensing 16, 851–876. doi:10.1080/01431169508954448.

Bell, T., Briggs, R., Bachmayer, R., Li, S., 2015. Augmenting Inuit knowledge for safe sea-ice travel - The SmartICE information system. 2014 Oceans - St. John's, OCEANS 2014 doi:10.1109/OCEANS.2014.7003290.

Benavent, N., Mahajan, A.S., Li, Q., Cuevas, C.A., Schmale, J., Angot, H., Jokinen, T., Quéléver, L.L., Blechschmidt, A.M., Zilker, B., Richter, A., Serna, J.A., Garcia-Nieto, D., Fernandez, R.P., Skov, H., Dumitrascu, A., Simões Pereira, P., Abrahamsson, K., Bucci, S., Duetsch, M., Stohl, A., Beck, I., Laurila, T., Blomquist, B., Howard, D., Archer, S.D., Bariteau, L., Helmig, D., Hueber, J., Jacobi, H.W., Posman, K., Dada, L., Daellenbach, K.R., Saiz-Lopez, A., 2022. Substantial contribution of iodine to Arctic ozone destruction. Nature Geoscience 2022 15:10 15, 770–773. doi:10.1038/s41561-022-01018-w.

Braakmann-Folgmann, A., Donlon, C., 2019. Estimating snow depth on Arctic sea ice using satellite microwave radiometry and a neural network. The Cryosphere 13, 2421–2438. doi:10.5194/tc-13-2421-2019.

Brandt, R.E., Warren, S.G., 1993. Solar-heating rates and temperature profiles in Antarctic snow and ice. Journal of Glaciology 39, 99–110. doi:10.3189/S0022143000015756.

Brucker, L., Markus, T., 2013. Arctic-scale assessment of satellite passive microwave-derived snow depth on sea ice using Operation IceBridge airborne data. Journal of Geophysical Research: Oceans 118, 2892–2905. doi:10.1002/jgrc.20228.

Cabaj, A., Kushner, P.J., Fletcher, C.G., Howell, S., Petty, A.A., 2020. Constraining Reanalysis Snowfall Over the Arctic Ocean Using CloudSat

Observations. Geophysical Research Letters 47, e2019GL086426. doi:10.1029/2019GL086426.

Cafarella, S.M., Scharien, R., Geldsetzer, T., Howell, S., Haas, C., Segal, R., Nasonova, S., 2019. Estimation of Level and Deformed First-Year Sea Ice Surface Roughness in the Canadian Arctic Archipelago from C- and L-Band Synthetic Aperture Radar. Canadian Journal of Remote Sensing 45, 457–475. doi:10.1080/07038992.2019.1647102.

Campbell, K., Lange, B.A., Landy, J.C., Katlein, C., Nicolaus, M., Anhaus, P., Matero, I., Gradinger, R., Charette, J., Duerksen, S., Tremblay, P., Rysgaard, S., Tranter, M., Haas, C., Michel, C., 2022. Net heterotrophy in High Arctic first-year and multi-year spring sea ice. Elementa 10. doi:10.1525/ELEMENTA.2021.00040/119112.

Campbell, K., Mundy, C.J., Barber, D.G., Gosselin, M., 2015. Characterizing the sea ice algae chlorophyll a–snow depth relationship over Arctic spring melt using transmitted irradiance. Journal of Marine Systems 147, 76–84. doi:10.1016/J.JMARSYS.2014.01.008.

Casey, J.A., Howell, S.E., Tivy, A., Haas, C., 2016. Separability of sea ice types from wide swath C- and L-band synthetic aperture radar imagery acquired during the melt season. Remote Sensing of Environment 174, 314–328. doi:10.1016/J.RSE.2015.12.021.

Castellani, G., Veyssière, G., Karcher, M., Stroeve, J., Banas, S.N., Bouman, A.H., Brierley, S.A., Connan, S., Cottier, F., Große, F., Hobbs, L., Katlein, C., Light, B., McKee, D., Orkney, A., Proud, R., Schourup-Kristensen, V., 2022. Shine a light: Under-ice light and its ecological implications in a changing Arctic Ocean. Ambio 51, 307–317. doi:10.1007/S13280-021-01662-3/FIGURES/5.

Chambellant, M., Stirling, I., Gough, W.A., Ferguson, S.H., 2012. Temporal variations in Hudson Bay ringed seal (Phoca hispida) life-history parameters in relation to environment. Journal of Mammalogy 93, 267–281. doi:10.1644/10-MAMM-A-253.1/2/JMAMMAL-93-1-267-FIG6.JPEG.

Clemens-Sewall, D., Polashenski, C., Frey, M.M., Cox, C.J., Granskog, M.A., Macfarlane, A.R., Fons, S.W., Schmale, J., Hutchings, J.K., von Albedyll, L., Arndt, S., Schneebeli, M., Perovich, D., 2023. Snow Loss Into Leads in Arctic Sea Ice: Minimal in Typical Wintertime Conditions, but High During a Warm and Windy Snowfall Event. Geophysical Research Letters 50, e2023GL102816. doi:10.1029/2023GL102816.

Colbeck, S.C., 1982. An overview of seasonal snow metamorphism. Reviews of Geophysics 20, 45–61. doi:10.1029/RG020i001p00045.

Colbeck, S.C., 1991. The layered character of snow covers. Reviews of Geophysics 29, 81–96. doi:10.1029/90RG02351.

Comiso, J.C., Cavalieri, D.J., Markus, T., 2003. Sea ice concentration, ice temperature, and snow depth using AMSR-E data. IEEE Transactions on Geoscience and Remote Sensing 41, 243–252. doi:10.1109/TGRS.2002.808317.

Confer, K.L., Jaeglé, L., Liston, G.E., Sharma, S., Nandan, V., Yackel, J., Ewert, M., Horowitz, H.M., 2023. Impact of Changing Arctic Sea Ice Extent, Sea Ice Age, and Snow Depth on Sea Salt Aerosol From Blowing Snow and the Open Ocean for 1980–2017. Journal of Geophysical Research: Atmospheres 128, e2022JD037667. doi:10.1029/2022JD037667.

Conger, S.M., McClung, D.M., 2009. Comparison of density cutters for snow profile observations. Journal of Glaciology 55, 163–169. doi:10.3189/002214309788609038.

Cota, G.F., 1985. Photoadaptation of high Arctic ice algae. Nature 1985 315:6016 315, 219–222. doi:10.1038/315219a0.

Cox, G.F., Weeks, W.F., 1974. Salinity Variations in Sea Ice. Journal of Glaciology 13, 109–120. doi:10.3189/S0022143000023418.

Crocker, G.B., 1984. A physical model for predicting the thermal conductivity of brine-wetted snow. Cold Regions Science and Technology 10, 69–74. doi:10.1016/0165-232X(84)90034-X.

Curry, J.A., Schramm, J.L., Ebert, E.E., 1995. Sea ice-albedo climate feedback mechanism. Journal of Climate 8. doi:10.1175/1520-0442(1995)008<0240:SIACFM>2.0.CO;2.

De Leeuw, G., Andreas, E.L., Anguelova, M.D., Fairall, C.W., Lewis, E.R., O'Dowd, C., Schulz, M., Schwartz, S.E., 2011. Production flux of sea spray aerosol. Reviews of Geophysics 49, 2001. doi:10.1029/2010RG000349.

De Montmollin, V., 1982. Shear Test on Snow Explained by Fast Metamorphism. Journal of Glaciology 28, 187–198. doi:10.3189/S0022143000011898.

De Rijke-Thomas, C., Landy, J., Mallett, R., Willatt, R., Tsamados, M., King, J., 2023. Airborne investigation of quasi-specular Ku-band radar scattering for satellite altimetry over snow-covered Arctic sea ice. IEEE Transactions on Geoscience and Remote Sensing , 1–1doi:10.1109/TGRS.2023.3318263.

Denoth, A., 1980. The Pendular-Funicular Liquid Transition in Snow. Journal of Glaciology 25, 93–98. doi:10.3189/S0022143000010315.

Denoth, A., 1982. The Pendular-Funicular Liquid Transition and Snow Metamorphism. Journal of Glaciology 28, 357–364. doi:10.3189/S0022143000011692.

Denoth, A., Foglar, A., 1985. Measurements of Daily Variations in the Subsurface Wetness Gradient. Annals of Glaciology 6, 254–255. doi:10.3189/S026030550001051X.

Dominé, F., Lauzier, T., Cabanes, A., Legagneux, L., Kuhs, W.F., Techmer, K., Heinrichs, T., 2003. Snow metamorphism as revealed by scanning electron microscopy. Microscopy Research and Technique 62, 33–48. doi:10.1002/JEMT.10384.

Dominé, F., Sparapani, R., Ianniello, A., Beine, H.J., 2004. The origin of sea salt in snow on Arctic sea ice and in coastal regions. Atmospheric Chemistry and Physics Discussions 4, 4737–4776. doi:10.5194/acpd-4-4737-2004.

Dominé, F., Taillandier, A.S., Cabanes, A., Douglas, T.A., Sturm, M., 2009. Three examples where the specific surface area of snow increased over time. Cryosphere 3, 31–39. doi:10.5194/TC-3-31-2009.

Drinkwater, M.R., Crocker, G.B., 1988. Modelling changes in the dielectric and scattering properties of young snow-covered sea ice at GHz frequencies. Journal of Glaciology 34, 274–282. doi:10.3189/s0022143000007012.

Drobot, S.D., Anderson, M.R., 2000. Spaceborne Microwave Remote Sensing of Arctic Sea Ice During Spring. Professional Geographer 52, 315–322. doi:10.1111/0033-0124.00227.

Durnford, D., Dastoor, A., 2011. The behavior of mercury in the cryosphere: A review of what we know from observations. Journal of Geophysical Research: Atmospheres 116, 6305. doi:10.1029/2010JD014809.

Edel, L., Claud, C., Genthon, C., Palerme, C., Wood, N., L'Ecuyer, T., Bromwich, D., 2020. Arctic Snowfall from ¡i¿CloudSat¡/i¿ Observations and Reanalyses. Journal of Climate 33, 2093–2109. doi:10.1175/JCLI-D-19-0105.1.

Ferguson, S., Taylor, M., Born, E., Rosing-Asvid, A., Messier, F., 2001. Activity and Movement Patterns of Polar Bears Inhabiting Consolidated versus Active Pack Ice. Arctic 54, 49–54.

Filhol, S., Sturm, M., 2015. Snow bedforms: A review, new data, and a formation model. Journal of Geophysical Research: Earth Surface 120, 1645–1669. doi:10.1002/2015JF003529.

Flocco, D., Feltham, D.L., Turner, A.K., 2010. Incorporation of a physically based melt pond scheme into the sea ice component of a climate model. Journal of Geophysical Research: Oceans 115, 8012. doi:10.1029/2009JC005568.

Flocco, D., Schroeder, D., Feltham, D.L., Hunke, E.C., 2012. Impact of melt ponds on Arctic sea ice simulations from 1990 to 2007. Journal of Geophysical Research: Oceans 117. doi:10.1029/2012JC008195.

Fors, A.S., Brekke, C., Gerland, S., Doulgeris, A.P., Beckers, J.F., 2016. Late Summer Arctic Sea Ice Surface Roughness Signatures in C-Band SAR Data. IEEE Journal of Selected Topics in Applied Earth Observations and Remote Sensing 9, 1199–1215. doi:10.1109/JSTARS.2015.2504384.

Fors, A.S., Divine, D.V., Doulgeris, A.P., Renner, A.H., Gerland, S., 2017. Signature of Arctic first-year ice melt pond fraction in X-band SAR imagery. Cryosphere 11, 755–771. doi:10.5194/TC-11-755-2017.

Fortier, M., Fortier, L., Michel, C., Legendre, L., 2002. Climatic and biological forcing of the vertical flux of biogenic particles under seasonal Arctic sea ice. Marine Ecology Progress Series 225, 1–16. doi:10.3354/MEPS225001.

Fox-Kemper, B., Hewitt, H., Xiao, C., Aoalgeirsdottir, G., Drijfhout, S., Edwards, T., Golledge, N., Hemer, M., Kopp, R., Krinner, G., Mix, A., Notz, D., Nowicki, S., Nurhati, I., Ruiz, I., Sallée, J.B., Slangen, A., Yu, Y., 2021. Ocean, Cryosphere and Sea Level Change, in: Masson-Delmotte V., Zhai P., Pirani A., Connors S.L., Péan C., Berger S., Caud N., Chen Y., Goldfarb L., Gomis M.I., Huang M., Leitzell K., Lonnoy E., Matthews J.B.R., Maycock T.K., Waterfield T., Yelekci O., Yuand R., Zhou B. (Eds.), Climate Change 2021: The Physical Science Basis. Contribution of Working Group I to the Sixth Assessment Report of the Intergovernmental Panel on Climate Change. Cambridge University Press, pp. 1211–1362.

Frey, K.E., Perovich, D.K., Light, B., 2011. The spatial distribution of solar radiation under a melting Arctic sea ice cover. Geophysical Research Letters 38. doi:10.1029/2011GL049421.

Frey, M.M., Norris, S.J., Brooks, I.M., Anderson, P.S., Nishimura, K., Yang, X., Jones, A.E., Nerentorp Mastromonaco, M.G., Jones, D.H., Wolff, E.W., 2020. First direct observation of sea salt aerosol production from blowing snow above sea ice. Atmospheric Chemistry and Physics 20, 2549–2578. doi:10.5194/ACP-20-2549-2020.

Fritsen, C.H., Lytle, V.I., Ackley, S.F., Sullivan, C.W., 1994. Autumn Bloom of Antarctic Pack-Ice Algae. Science 266, 782–784. doi:10.1126/SCIENCE.266.5186.782.

Gardner, A.S., Sharp, M.J., 2010. A review of snow and ice albedo and the development of a new physically based broadband albedo parameterization. Journal of Geophysical Research: Earth Surface 115. doi:10.1029/2009JF001444.

Garnier, F., Fleury, S., Garric, G., Bouffard, J., Tsamados, M., Laforge, A., Bocquet, M., Fredensborg Hansen, R.M., Remy, F., 2021. Advances in altimetric snow depth estimates using bi-frequency SARAL and CryoSat-2 Ka–Ku measurements. The Cryosphere 15, 5483–5512. doi:10.5194/TC-15-5483-2021.

Gay, M., Fily, M., Genthon, C., Frezzotti, M., Oerter, H., Winther, J.G.G., 2002. Snow grain-size measurements in Antarctica. Journal of Glaciology 48, 527–535. doi:10.3189/172756502781831016.

Geldsetzer, T., Langlois, A., Yackel, J., 2009. Dielectric properties of brine-wetted snow on first-year sea ice. Cold Regions Science and Technology 58, 47–56. doi:10.1016/j.coldregions.2009.03.009.

Geldsetzer, T., Mead, J.B., Yackel, J.J., Scharien, R.K., Howell, S.E., 2007. Surface-based polarimetric C-band scatterometer for field measurements of sea ice. IEEE Transactions on Geoscience and Remote Sensing 45, 3405–3416. doi:10.1109/TGRS.2007.907043.

Geldsetzer, T., Yackel, J., Tomar, K.S., Mahmud, M., Nandan, V., Kumar, S., 2023. Melt pond detection on landfast sea ice using dual co-polarized Ku-band backscatter. Remote Sensing of Environment 296, 113725. doi:10.1016/J.RSE.2023.113725.

Glissenaar, I.A., Landy, J.C., Petty, A.A., Kurtz, N.T., Stroeve, J.C., 2021. Impacts of snow data and processing methods on the interpretation of long-term changes in Baffin Bay sea ice thickness. The Cryosphere Discussions 2021, 1–26. doi:10.5194/tc-2021-135.

Golden, K.M., Ackley, S.F., Lytle, V.I., 1998. The percolation phase transition in sea ice. Science 282, 2238–2241. doi:10.1126/science.282.5397.2238.

Gong, X., Zhang, J., Croft, B., Yang, X., Frey, M.M., Bergner, N., Chang, R.Y., Creamean, J.M., Kuang, C., Martin, R.V., Ranjithkumar, A., Sedlacek, A.J., Uin, J., Willmes, S., Zawadowicz, M.A., Pierce, J.R., Shupe, M.D., Schmale, J., Wang, J., 2023. Arctic warming by abundant fine sea salt aerosols from blowing snow. Nature Geoscience 2023 16:9 16, 768–774. doi:10.1038/s41561-023-01254-8.

Gosselin, M., Legendre, L., Therriault, J.C., Demers, S., Rochet, M., 1986. Physical control of the horizontal patchiness of sea-ice microalgae. Marine Ecology Progress Series 29, 289–298.

Gradinger, R., Spindler, M., Henschel, D., 1991. Development of Arctic sea-ice organisms under graded snow cover. Polar Research 10. doi:10.3402/polar.v10i1.6748.

Graham, R.M., Cohen, L., Petty, A.A., Boisvert, L.N., Rinke, A., Hudson, S.R., Nicolaus, M., Granskog, M.A., 2017. Increasing frequency and duration of Arctic winter warming events. Geophysical Research Letters 44, 6974–6983.

Grannas, A.M., Jones, A.E., Dibb, J., Ammann, M., Anastasio, C., Beine, H.J., Bergin, M., Bottenheim, J., Boxe, C.S., Carver, G., Chen, G., Crawford, J.H., Dominé, F., Frey, M.M., Guzmán, M.I., Heard, D.E., Helmig, D., Hoffmann, M.R., Honrath, R.E., Huey, L.G., Hutterli, M., Jacobi, H.W., Klán, P., Lefer, B., McConnell, J., Plane, J., Sander, R., Savarino, J., Shepson, P.B., Simpson, W.R., Sodeau, J.R., Von Glasow, R., Weller, R., Wolff, E.W., Zhu, T., 2007. An overview of snow photochemistry: Evidence, mechanisms and impacts. Atmospheric Chemistry and Physics 7, 4329–4373. doi:10.5194/ACP-7-4329-2007.

Granskog, M.A., Assmy, P., Koç, N., 2019. Emerging traits of sea ice in the Atlantic sector of the Arctic. Climate Change and the White World , 3–10doi:10.1007/978-3-030-21679-5{_}1/COVER.

Granskog, M.A., Kaartokallio, H., Kuosa, H., Thomas, D.N., Ehn, J., Sonninen, E., 2005. Scales of horizontal patchiness in chlorophyll a, chemical and physical properties of landfast sea ice in the Gulf of Finland (Baltic Sea). Polar Biology 28, 276–283. doi:10.1007/S00300-004-0690-5/FIGURES/3.

Granskog, M.A., Rösel, A., Dodd, P.A., Divine, D., Gerland, S., Martma, T., Leng, M.J., 2017. Snow contribution to first-year and second-year Arctic sea ice mass balance north of Svalbard. Journal of Geophysical Research: Oceans 122, 2539–2549. doi:10.1002/2016JC012398@10.1002/(ISSN)2169-9291.NICE1.

Granskog, M.A., Vihma, T., Pirazzini, R., Cheng, B., 2006. Superimposed ice formation and surface energy fluxes on sea ice during the spring melt-freeze period in the Baltic Sea. Journal of Glaciology 52, 119–127. doi:10.3189/172756506781828971.

Grenfell, T.C., Perovich, D.K., 2004. Seasonal and spatial evolution of albedo in a snow-ice-land-ocean environment. Journal of Geophysical Research: Oceans 109. doi:10.1029/2003JC001866.

Grossi, S.M., Kottmeier, S.T., Moe, R.L., Taylor, G.T., Sullivan, C.W., 1987. Sea ice microbial communities. VI. Growth and primary production in bottom ice under graded snow cover. Marine Ecology Progress Series , 153–164.

Guarino, M.V., Sime, L.C., Schröeder, D., Malmierca-Vallet, I., Rosenblum, E., Ringer, M., Ridley, J., Feltham, D., Bitz, C., Steig, E.J., Wolff, E., Stroeve, J., Sellar, A., 2020. Sea-ice-free Arctic during the Last Interglacial supports fast future loss. Nature Climate Change 2020 10:10 10, 928–932. doi:10.1038/s41558-020-0865-2.

Guerreiro, K., Fleury, S., Zakharova, E., Rémy, F., Kouraev, A., 2016. Potential for estimation of snow depth on Arctic sea ice from CryoSat-2 and SARAL/AltiKa missions. Remote Sensing of Environment 186, 339–349. doi:10.1016/j.rse.2016.07.013.

Haas, C., Thomas, D.N., Bareiss, J., 2001. Surface properties and processes of perennial Antarctic sea ice in summer. Journal of Glaciology 47, 613–625. doi:10.3189/172756501781831864.

Hallikainen, M.T., Ulaby, F.T., Van Deventer, T.E., 1987. Extinction Behavior of Dry Snow in the 18- to 90-GHz Range. IEEE Transactions on Geoscience and Remote Sensing GE-25, 737–745. doi:10.1109/TGRS.1987.289743.

Hammill, M.O., Smith, T.G., 2011. Factors affecting the distribution and abundance of ringed seal structures in Barrow Strait, Northwest Territories. https://doi.org/10.1139/z89-312 67, 2212–2219. doi:10.1139/Z89-312.

Hancke, K., Lund-Hansen, L.C., Lamare, M.L., Højlund Pedersen, S., King, M.D., Andersen, P., Sorrell, B.K., 2018. Extreme Low Light Requirement for Algae Growth Underneath Sea Ice: A Case Study From Station Nord, NE Greenland. Journal of Geophysical Research: Oceans 123, 985–1000. doi:10.1002/2017JC013263.

Hauser, D.D., Frost, K.J., Burns, J.J., 2023. Predation on ringed seals in subnivean lairs in northwest Alaska during spring 1983 and 1984. Marine Mammal Science 39, 311–321. doi:10.1111/MMS.12969.

Hezel, P.J., Zhang, X., Bitz, C.M., Kelly, B.P., Massonnet, F., 2012. Projected decline in spring snow depth on Arctic sea ice caused by progressively later autumn open ocean freeze-up this century. Geophysical Research Letters 39, n/a–n/a. doi:10.1029/2012GL052794.

Holland, M.M., Landrum, L., 2021. The Emergence and Transient Nature of Arctic Amplification in Coupled Climate Models. Frontiers in Earth Science 9, 764. doi:10.3389/FEART.2021.719024/BIBTEX.

Holtsmark, B.E., 1955. Insulating Effect of a Snow Cover on the Growth of Young Sea Ice. Arctic 8, 60–65.

Hov, ., Shepson, P., Wolff, E., 2007. The chemical composition of the polar atmosphere–The IPY contribution. Bulletin of the World Meteorological Organization , 263–269.

Howell, S.E., Small, D., Rohner, C., Mahmud, M.S., Yackel, J.J., Brady, M., 2019. Estimating melt onset over Arctic sea ice from time series multi-sensor Sentinel-1 and RADARSAT-2 backscatter. Remote Sensing of Environment 229, 48–59. doi:10.1016/J.RSE.2019.04.031.

Howell, S.E., Yackel, J.J., De Abreu, R., Geldsetzer, T., Breneman, C., 2005. On the utility of SeaWinds/QuikSCAT data for the estimation of the thermodynamic state of first-year sea ice. IEEE Transactions on Geoscience and Remote Sensing 43, 1338–1350. doi:10.1109/TGRS.2005.846153.

Hu, Y., Lu, X., Zeng, X., Stamnes, S.A., Neuman, T.A., Kurtz, N.T., Zhai, P., Gao, M., Sun, W., Xu, K., Liu, Z., Omar, A.H., Baize, R.R., Rogers, L.J., Mitchell, B.O., Stamnes, K., Huang, Y., Chen, N., Weimer, C., Lee, J., Fair, Z., 2022. Deriving Snow Depth From ICESat-2 Lidar Multiple Scattering Measurements. Frontiers in Remote Sensing 3, 855159. doi:10.3389/FRSEN.2022.855159.

Huang, L., Fischer, G., Hajnsek, I., 2021. Antarctic snow-covered sea ice topography derivation from TanDEM-X using polarimetric SAR interferometry. Cryosphere 15, 5323–5344. doi:10.5194/TC-15-5323-2021.

Hvidegaard, S., Forsberg, F., Skourup, H., Kristensen, M., Olesen, A., Olesen, A., Coccia, A., Macedo, K., Helm, V., Ladkin, R., Tilling, R., Hogg, A., Lemos, A., Shepherd, A., 2020. ESA CryoVEx/KAREN Antarctica 2017-18. Technical Report. DTU Space.

Iacozza, J., Barber, D.G., 1999. An examination of the distribution of snow on sea-ice. Atmosphere - Ocean 37, 21–51. doi:10.1080/07055900.1999.9649620.

Isleifson, D., Galley, R.J., Barber, D.G., Landy, J.C., Komarov, A.S., Shafai, L., 2014. A study on the c-band polarimetric scattering and physical characteristics of frost flowers on experimental sea ice. IEEE Transactions on Geoscience and Remote Sensing 52, 1787–1798. doi:10.1109/TGRS.2013.2255060.

Istomina, L., Heygster, G., Huntemann, M., Schwarz, P., Birnbaum, G., Scharien, R., Polashenski, C., Perovich, D., Zege, E., Malinka, A., Prikhach, A., Katsev, I., 2015. Melt pond fraction and spectral sea ice albedo retrieval from MERIS data - Part 1: Validation against in situ, aerial, and ship cruise data. Cryosphere 9, 1551–1566. doi:10.5194/TC-9-1551-2015.

Itkin, P., Webster, M., Hendricks, S., Oggier, M., Jaggi, M., Ricker, R., Arndt, S., Divine, D.V., von Albedyll, L., Raphael, I., Rohde, J., Liston, G.E., 2021. Magnaprobe snow and melt pond depth measurements from the 2019-2020 MOSAiC expedition.

Jeffries, M.O., Krouse, H.R., Hurst-Cushing, B., Maksym, T., 2001. Snow-ice accretion and snow-cover depletion on Antarctic first-year sea-ice floes. Annals of Glaciology 33, 51–60. doi:10.3189/172756401781818266.

Jutila, A., Hendricks, S., Ricker, R., Von Albedyll, L., Krumpen, T., Haas, C., 2022. Retrieval and parameterisation of sea-ice bulk density from airborne multi-sensor measurements. Cryosphere 16, 259–275. doi:10.5194/TC-16-259-2022.

Jutras, M., Vancoppenolle, M., Lourenço, A., Vivier, F., Carnat, G., Madec, G., Rousset, C., Tison, J.L., 2016. Thermodynamics of slush and snow–ice formation in the Antarctic sea-ice zone. Deep-Sea Research Part II: Topical Studies in Oceanography 131, 75–83. doi:10.1016/j.dsr2.2016.03.008.

Kaltenborn, J., Macfarlane, A.R., Clay, V., Schneebeli, M., 2023. Automatic snow type classification of snow micropenetrometer profiles with machine learning algorithms. Geoscientific Model Development 16, 4521–4550. doi:10.5194/GMD-16-4521-2023.

Kane, D.L., Gieck, R.E., Hinzman, L.D., 1997. Snowmelt Modeling at Small Alaskan Arctic Watershed. Journal of Hydrologic Engineering 2, 204–210. doi:10.1061/(ASCE)1084-0699(1997)2:4(204).

Kari, E., Jutila, A., Friedrichs, A., Lepparanta, M., Kratzer, S., 2020. Measurements of light transfer through drift ice and landfast ice in the northern Baltic Sea. Oceanologia 62, 347–363. doi:10.1016/J.OCEANO.2020.04.001.

Katlein, C., Arndt, S., Belter, H.J., Castellani, G., Nicolaus, M., 2019. Seasonal Evolution of Light Transmission Distributions Through Arctic Sea Ice. Journal of Geophysical Research: Oceans 124, 5418–5435. doi:10.1029/2018JC014833.

Kawamura, T., Jeffries, M.O., Tison, J.L., Krouse, H.R., 2004. Superimposed-ice formation in summer on Ross Sea pack-ice floes. Annals of Glaciology 39, 563–568. doi:10.3189/172756404781814168.

Kern, M., Cullen, R., Berruti, B., Bouffard, J., Casal, T., Drinkwater, M.R., Gabriele, A., Lecuyot, A., Ludwig, M., Midthassel, R., Navas Traver, I., Parrinello, T., Ressler, G., Andersson, E., Martin-Puig, C., Andersen, O., Bartsch, A., Farrell, S., Fleury, S., Gascoin, S., Guillot, A., Humbert, A., Rinne, E., Shepherd, A., van den Broeke, M.R., Yackel, J., 2020. The Copernicus Polar Ice and Snow Topography Altimeter (CRISTAL) high-priority candidate mission. The Cryosphere 14, 2235–2251. doi:10.5194/tc-14-2235-2020.

Kern, S., Spreen, G., 2015. Uncertainties in Antarctic sea-ice thickness retrieval from ICESat. Annals of Glaciology 56, 107–119. doi:10.3189/2015AOG69A736.

King, J., Howell, S., Brady, M., Toose, P., Derksen, C., Haas, C., Beckers, J., 2020. Local-scale variability of snow density on Arctic sea ice. The Cryosphere 14, 4323–4339. doi:10.5194/tc-14-4323-2020.

King, J., Howell, S., Derksen, C., Rutter, N., Toose, P., Beckers, J.F., Haas, C., Kurtz, N., Richter-Menge, J., 2015a. Evaluation of Operation IceBridge quick-look snow depth estimates on sea ice. Geophysical Research Letters 42, 9302–9310. doi:10.1002/2015GL066389.

King, J., Kelly, R., Kasurak, A., Duguay, C., Gunn, G., Rutter, N., Watts, T., Derksen, C., 2015b. Spatio-temporal influence of tundra snow properties on Ku-band (17.2 GHz) backscatter. Journal of Glaciology 61, 267–279. doi:10.3189/2015JOG14J020.

King, J., Skourup, H., Hvidegaard, S.M., Rösel, A., Gerland, S., Spreen, G., Polashenski, C., Helm, V., Liston, G.E., 2018. Comparison of Freeboard Retrieval and Ice Thickness Calculation From ALS, ASIRAS, and CryoSat-2 in the Norwegian Arctic to Field Measurements Made During the N-ICE2015 Expedition. Journal of Geophysical Research: Oceans 123, 1123–1141. doi:10.1002/2017JC013233.

King, J.M., Kelly, R., Kasurak, A., Duguay, C., Gunn, G., Mead, J.B., 2013. UW-Scat: A ground-based dual-frequency scatterometer for observation of snow properties. IEEE Geoscience and Remote Sensing Letters 10, 528–532. doi:10.1109/LGRS.2012.2212177.

Kingsley, M.C., Hammill, M.O., Kelly, B.P., 1990. INFRARED SENSING OF THE UNDER-SNOW LAIRS OF THE RINGED SEAL. Marine Mammal Science 6, 339–347. doi:10.1111/J.1748-7692.1990.TB00363.X.

Köck, G., Triendl, M., Hofer, R., 1996. Seasonal patterns of metal accumulation in Arctic char (Salvelinus alpinus) from an oligotrophic Alpine lake related to temperature. Canadian Journal of Fisheries and Aquatic Sciences 53. doi:10.1139/f95-243.

Koscielny-Bunde, E., Kantelhardt, J.W., Braun, P., Bunde, A., Havlin, S., 2006. Long-term persistence and multifractality of river runoff records: Detrended fluctuation studies. Journal of Hydrology 322, 120–137. doi:10.1016/J.JHYDROL.2005.03.004.

Krupnik, I., Aporta, C., Laidler, G.J., Gearheard, S., Holm, L.K., 2010. SIKU: Knowing our ice: Documenting Inuit sea ice knowledge and use. SIKU: Knowing Our Ice: Documenting Inuit Sea Ice Knowledge and Use , 1–501doi:10.1007/978-90-481-8587-0/COVER.

Kurtz, N.T., Farrell, S.L., 2011. Large-scale surveys of snow depth on Arctic sea ice from Operation IceBridge. Geophysical Research Letters 38. doi:10.1029/2011GL049216.

Kurtz, N.T., Farrell, S.L., Studinger, M., Galin, N., Harbeck, J.P., Lindsay, R., Onana, V.D., Panzer, B., Sonntag, J.G., 2013. Sea ice thickness, freeboard, and snow depth products from Operation IceBridge airborne data. Cryosphere 7, 1035–1056. doi:10.5194/tc-7-1035-2013.

Kwok, R., Cunningham, G.F., 2008. ICESat over Arctic sea ice: Estimation of snow depth and ice thickness. Journal of Geophysical Research: Oceans 113, C08010. doi:10.1029/2008JC004753.

Kwok, R., Haas, C., 2015. Effects of radar side-lobes on snow depth retrievals from Operation IceBridge. Journal of Glaciology 61. doi:10.3189/2015JoG14J229.

Kwok, R., Kacimi, S., Webster, M.A., Kurtz, N.T., Petty, A.A., 2020. Arctic Snow Depth and Sea Ice Thickness From ICESat-2 and CryoSat-2 Freeboards: A First Examination. Journal of Geophysical Research: Oceans 125, 1–19. doi:10.1029/2019JC016008.

Kwok, R., Kurtz, N.T., Brucker, L., Ivanoff, A., Newman, T., Farrell, S.L., King, J., Howell, S., Webster, M.A., Paden, J., Leuschen, C., MacGregor, J.A., Richter-Menge, J., Harbeck, J., Tschudi, M., 2017. Intercomparison of snow depth retrievals over Arctic sea ice from radar data acquired by Operation IceBridge. Cryosphere 11, 2571–2593. doi:10.5194/tc-11-2571-2017.

Kwok, R., Maksym, T., 2014. Snow depth of the Weddell and Bellingshausen sea ice covers from IceBridge surveys in 2010 and 2011: An examination. doi:10.1002/2014JC009943.

Laidler, G.J., Ford, J.D., Gough, W.A., Ikummaq, T., Gagnon, A.S., Kowal, S., Qrunnut, K., Irngaut, C., 2009. Travelling and hunting in a changing Arctic: Assessing Inuit vulnerability to sea ice change in Igloolik, Nunavut. Climatic Change 94, 363–397. doi:10.1007/S10584-008-9512-Z/METRICS.

Landy, J.C., Tsamados, M., Scharien, R.K., 2019. A Facet-Based Numerical Model for Simulating SAR Altimeter Echoes from Heterogeneous Sea Ice Surfaces. IEEE Transactions on Geoscience and Remote Sensing 57, 4164–4180. doi:10.1109/TGRS.2018.2889763.

Lange, B.A., Haas, C., Charette, J., Katlein, C., Campbell, K., Duerksen, S., Coupel, P., Anhaus, P., Jutila, A., Tremblay, O., Carlyle, C.G., Michel, C., 2019. Contrasting Ice Algae and Snow-Dependent Irradiance Relationships Between First-Year and Multiyear Sea Ice. Geophysical Research Letters 46, 10834–10843. doi:10.1029/2019GL082873.

Lange, M.A., Schlosser, P., Ackley, S.F., Wadhams, P., Dieckmann, G.S., 1990. 18O Concentrations In Sea Ice Of The Weddell Sea, Antarctica. Journal of Glaciology 36, 315–323. doi:10.3189/002214390793701291.

Langlois, A., Mundy, C., Barber, D.G., 2007. On the winter evolution of snow thermophysical properties over land-fast first-year sea ice. Hydrological Processes: An International Journal 21, 705–716.

Larue, F., Picard, G., Aublanc, J., Arnaud, L., Robledano-Perez, A., LE Meur, E., Favier, V., Jourdain, B., Savarino, J., Thibaut, P., 2021. Radar altimeter waveform simulations in Antarctica with the Snow Microwave Radiative Transfer Model (SMRT). Remote Sensing of Environment 263, 112534. doi:10.1016/J.RSE.2021.112534.

Launiainen, J., Cheng, B., 1998. Modelling of ice thermodynamics in natural water bodies. Cold Regions Science and Technology 27, 153–178.

Lawrence, I.R., Tsamados, M.C., Stroeve, J.C., Armitage, T.W., Ridout, A.L., 2018. Estimating snow depth over Arctic sea ice from calibrated dual-frequency radar freeboards. Cryosphere 12, 3551–3564. doi:10.5194/tc-12-3551-2018.

Lebrun, M., Vancoppenolle, M., Madec, G., Babin, M., Becu, G., Lourenço, A., Nomura, D., Vivier, F., Delille, B., 2023. Light Under Arctic Sea Ice in Observations and Earth System Models. Journal of Geophysical Research: Oceans 128, e2021JC018161. doi:10.1029/2021JC018161.

Lecomte, O., Fichefet, T., Vancoppenolle, M., Domine, F., Massonnet, F., Mathiot, P., Morin, S., Barriat, P., 2013. On the formulation of snow thermal conductivity in large-scale sea ice models. Journal of Advances in Modeling Earth Systems 5, 542–557. doi:10.1002/JAME.20039.

Ledley, T.S., 1991. Snow on sea ice: competing effects in shaping climate. Journal of Geophysical Research 96, 17195–17208. doi:10.1029/91jd01439.

Ledley, T.S., 1993. Variations in snow on sea ice: a mechanism for producing climate variations. Journal of Geophysical Research 98, 10401–10410. doi:10.1029/93jd00316.

Lee, S.M., Shi, H., Sohn, B.J., Gasiewski, A.J., Meier, W.N., Dybkjær, G., 2021. Winter Snow Depth on Arctic Sea Ice From Satellite Radiometer Measurements (2003–2020): Regional Patterns and Trends. Geophysical Research Letters 48, e2021GL094541. doi:10.1029/2021GL094541.

Lei, Y.D., Wania, F., 2004. Is rain or snow a more efficient scavenger of organic chemicals? Atmospheric Environment 38, 3557–3571. doi:10.1016/J.ATMOSENV.2004.03.039.

Letcher, T., Parno, J., Courville, Z., Farnsworth, L., Olivier, J., 2022. A generalized photon-tracking approach to simulate spectral snow albedo and transmittance using X-ray microtomography and geometric optics. Cryosphere 16, 4343–4361. doi:10.5194/TC-16-4343-2022.

Leu, E., Mundy, C.J., Assmy, P., Campbell, K., Gabrielsen, T.M., Gosselin, M., Juul-Pedersen, T., Gradinger, R., 2015. Arctic spring awakening – Steering principles behind the phenology of vernal ice algal blooms. Progress in Oceanography 139, 151–170. doi:10.1016/J.POCEAN.2015.07.012.

Leu, E., Søreide, J.E., Hessen, D.O., Falk-Petersen, S., Berge, J., 2011. Consequences of changing sea-ice cover for primary and secondary producers in the European Arctic shelf seas: Timing, quantity, and quality. Progress in Oceanography 90, 18–32. doi:10.1016/J.POCEAN.2011.02.004.

Libois, Q., Picard, G., France, J.L., Arnaud, L., Dumont, M., Carmagnola, C.M., King, M.D., 2013. Influence of grain shape on light penetration in snow. Cryosphere 7, 1803–1818. doi:10.5194/TC-7-1803-2013.

Light, B., Smith, M.M., Perovich, D.K., Webster, M.A., Holland, M.M., Linhardt, F., Raphael, I.A., Clemens-Sewall, D., Macfarlane, A.R., Anhaus, P., Bailey, D.A., 2022. Arctic sea ice albedo: Spectral composition, spatial heterogeneity, and temporal evolution observed during the MOSAiC drift. Elementa 10. doi:10.1525/ELEMENTA.2021.000103/190677.

Lindsay, J.M., Hauser, D.D.W., Mahoney, A.R., Laidre, K.L., Goodwin, J., Harris, C., Schaeffer, R.J., Sr., R.S., Whiting, A.V., Boveng, P.L., Laxague, N.J.M., Betcher, S., Subramaniam, A., Witte, C.R., Zappa, C.J., 2023. Characteristics of ringed seal Pusa hispida ('natchiq') denning habitat in Kotzebue Sound, Alaska, during a year of limited sea ice and snow. Marine Ecology Progress Series 705, 1–20. doi:10.3354/MEPS14252.

Lindsay, J.M., Laidre, K.L., Conn, P.B., Moreland, E.E., Boveng, P.L., 2021. Modeling ringed seal Pusa hispida habitat and lair emergence timing in the eastern Bering and Chukchi Seas. Endangered Species Research 46, 1–17. doi:10.3354/ESR01140.

Liston, G.E., Itkin, P., Stroeve, J., Tschudi, M., Stewart, J.S., Pedersen, S.H., Reinking, A.K., Elder, K., 2020. A Lagrangian Snow-Evolution System for Sea-Ice Applications (SnowModel-LG): Part I – Model Description. Journal of Geophysical Research: Oceans 125, e2019JC015913. doi:10.1029/2019jc015913.

Liston, G.E., Polashenski, C., Rösel, A., Itkin, P., King, J., Merkouriadi, I., Haapala, J., 2018. A Distributed Snow-Evolution Model for Sea-Ice Applications (SnowModel). Journal of Geophysical Research: Oceans 123, 3786–3810. doi:10.1002/2017JC013706.

Lombardo, M., Schneebeli, M., Lowe, H., 2021. A casting method using contrast-enhanced diethylphthalate for micro-computed tomography of snow. Journal of Glaciology 67, 847–861.

Lund-Hansen, L.C., Hawes, I., Hancke, K., Salmansen, N., Nielsen, J.R., Balslev, L., Sorrell, B.K., 2020. Effects of increased irradiance on biomass, photobiology, nutritional quality, and pigment composition of Arctic sea ice algae. Marine Ecology Progress Series 648. doi:10.3354/meps13411.

Lüthje, M., Feltham, D.L., Taylor, P.D., Worster, M.G., 2006. Modeling the summertime evolution of sea-ice melt ponds. Journal of Geophysical Research: Oceans 111, 2001. doi:10.1029/2004JC002818.

Macfarlane, A.R., Dadic, R., Smith, M.M., Light, B., Nicolaus, M., Henna-Reetta, H., Webster, M., Linhardt, F., Hämmerle, S., Schneebeli, M., 2023a. Evolution of the microstructure and reflectance of the surface scattering layer on melting, level Arctic sea ice. Elementa 11. doi:10.1525/ELEMENTA.2022.00103/195863.

Macfarlane, A.R., L{\"o}we, H., Gimenes, L., Wagner, D.N., Dadic, R., Ottersberg, R., H{\"a}mmerle, S., Schneebeli, M., 2023b. Thermal Conductivity of Snow on Arctic Sea Ice. The Cryosphere Discussions , 1–22.

Mahmud, M.S., Howell, S.E., Geldsetzer, T., Yackel, J., 2016. Detection of melt onset over the northern Canadian Arctic Archipelago sea ice from RADARSAT, 1997–2014. Remote Sensing of Environment 178, 59–69. doi:10.1016/J.RSE.2016.03.003.

Mahmud, M.S., Nandan, V., Howell, S.E., Geldsetzer, T., Yackel, J., 2020. Seasonal evolution of L-band SAR backscatter over landfast Arctic sea ice. Remote Sensing of Environment 251, 112049. doi:10.1016/J.RSE.2020.112049.

Mahoney, A.R., Turner, K.E., Hauser, D.D., Laxague, N.J., Lindsay, J.M., Whiting, A.V., Witte, C.R., Goodwin, J., Harris, C., Schaeffer, R.J., Schaeffer, R., Betcher, S., Subramaniam, A., Zappa, C.J., 2021. Thin ice, deep snow and surface flooding in Kotzebue Sound: landfast ice mass balance during two anomalously warm winters and implications for marine mammals and subsistence hunting. Journal of Glaciology 67, 1013–1027. doi:10.1017/JOG.2021.49.

Maksym, T., Jeffries, M.O., 2000. A one-dimensional percolation model of flooding and snow ice formation on Antarctic sea ice. Journal of Geophysical Research: Oceans 105, 26313–26331. doi:10.1029/2000JC900130.

Malinka, A., Zege, E., Heygster, G., Istomina, L., 2016. Reflective properties of white sea ice and snow. Cryosphere 10, 2541–2557. doi:10.5194/tc-10-2541-2016.

Mallett, R., 2021. Snow structure with the snow crystal card. Nature Reviews Earth & Environment 2021 2:3 2, 165–165. doi:10.1038/s43017-021-00149-9.

Mallett, R.D.C., Lawrence, I.R., Stroeve, J.C., Landy, J.C., Tsamados, M., 2020. Brief communication: Conventional assumptions involving the speed of radar waves in snow introduce systematic underestimates to sea ice thickness and seasonal growth rate estimates. Cryosphere 14, 251–260. doi:10.5194/tc-14-251-2020.

Mallett, R.D.C., Stroeve, J.C., Tsamados, M., Willatt, R., Newman, T., Nandan, V., Landy, J.C., Itkin, P., Oggier, M., Jaggi, M., Perovich, D., 2022. Sub-kilometre scale distribution of snow depth on Arctic sea ice from Soviet drifting stations. Journal of Glaciology , 1–13doi:10.1017/JOG.2022.18.

{{Maritime Executive}}, 2022. Cruise Ship Assists Britain's Attenborough Due to Difficult Sea Ice.

Marks, A.A., King, M.D., 2014. The effect of snow/sea ice type on the response of albedo and light penetration depth (ie-folding depth) to increasing black carbon. Cryosphere 8, 1625–1638. doi:10.5194/TC-8-1625-2014.

Markus, T., Cavalieri, D.J., 1998. Snow depth distribution over sea ice in the Southern Ocean from satellite passive microwave data. Antarctic sea ice: physical processes, interactions and variability 74, 19–39. doi:10.1029/ar074p0019.

Markus, T., Stroeve, J.C., Miller, J., 2009. Recent changes in Arctic sea ice melt onset, freezeup, and melt season length. Journal of Geophysical Research: Oceans 114, C12024. doi:10.1029/2009JC005436.

Martin, J., Schneebeli, M., 2023. Impact of the sampling procedure on the specific surface area of snow measurements with the IceCube. Cryosphere 17, 1723–1734. doi:10.5194/TC-17-1723-2023.

Massom, R.A., Eicken, H., Haas, C., Jeffries, M.O., Drinkwater, M.R., Sturm, M., Worby, A.P., Wu, X., Lytle, V.I., Ushio, S., Morris, K., Reid, P.A., Warren, S.G., Allison, I., 2001. Snow on Antarctic sea ice. Reviews of Geophysics 39, 413–445. doi:10.1029/2000RG000085.

Matzl, M., Schneebeli, M., 2006. Measuring specific surface area of snow by near-infrared photography. Journal of Glaciology 52, 558–564. doi:10.3189/172756506781828412.

Maykut, G.A., Untersteiner, N., MAYKUT GA, UNTERSTEINER N, 1971. Some results from a time- dependent thermodynamic model of sea ice. J Geophys Res 76, 1550–1575. doi:10.1029/jc076i006p01550.

McCrystall, M.R., Stroeve, J., Serreze, M., Forbes, B.C., Screen, J.A., 2021. New climate models reveal faster and larger increases in Arctic precipitation than previously projected. Nature Communications 2021 12:1 12, 1–12. doi:10.1038/s41467-021-27031-y.

Meier, W.N., Markus, T., Comiso, J.C., 2018. AMSR-E/AMSR2 Unified L3 Daily 12.5 km Brightness Temperatures, Sea Ice Concentration, Motion & Snow Depth Polar Grids, Version 1. NASA National Snow and Ice Data Center Distributed Active Archive Center doi:doi.org/10.5067/RA1MIJOYPK3P.

Meredith, M., Sommerkorn, M., Cassotta, S., Derksen, C., Ekaykin, A., Hollowed, A., Kofinas, G., Mackintosh, A., Melbourne-Thomas, J., Muelbert, M., Ottersen, G., Pritchard, H., Schuur, E., 2019. Polar Regions, in: Portner, H.O., Roberts, D., Masson-Delmotte, V., Zhai, P., Tignor, M., Poloczanska, E., Mintenbeck, K., Alegria, A., Nicolai, M., Okem, A., Petzold, J., Rama, B., Weyer, N. (Eds.), IPCC Special Report on the Ocean and Cryosphere in a Changing Climate. IPCC, pp. 203–320.

Merkouriadi, I., Liston, G.E., Graham, R.M., Granskog, M.A., 2020. Quantifying the Potential for Snow-Ice Formation in the Arctic Ocean. Geophysical Research Letters 47, e2019GL085020. doi:10.1029/2019GL085020.

Meyer, T., Wania, F., 2008. Organic contaminant amplification during snowmelt. Water Research 42, 1847–1865. doi:10.1016/J.WATRES.2007.12.016.

Michel, C., Legendre, L., Demers, S., Therriault, J.C., 1988. Photoadaptation of sea-ice microalgae in springtime: photosynthesis and carboxylating enzymes. Marine Ecology Progress Series 50, 177–185.

Moon, W., Nandan, V., Scharien, R.K., Wilkinson, J., Yackel, J.J., Barrett, A., Lawrence, I., Segal, R.A., Stroeve, J., Mahmud, M., Duke, P.J., Else, B., 2019. Physical length scales of wind-blown snow redistribution and accumulation on relatively smooth Arctic first-year sea ice. Environmental Research Letters 14, 104003. doi:10.1088/1748-9326/ab3b8d.

Mundy, C.J., Barber, D.G., Michel, C., 2005. Variability of snow and ice thermal, physical and optical properties pertinent to sea ice algae biomass during spring. Journal of Marine Systems 58, 107–120. doi:10.1016/j.jmarsys.2005.07.003.

Mundy, C.J., Gosselin, M., Gratton, Y., Brown, K., Galindo, V., Campbell, K., Levasseur, M., Barber, D., Papakyriakou, T., Bélanger, S., 2014. Role of environmental factors on phytoplankton bloom initiation under landfast sea ice in Resolute Passage, Canada. Marine Ecology Progress Series 497, 39–49. doi:10.3354/MEPS10587.

Nab, C., Mallett, R., Gregory, W., Landy, J., Lawrence, I., Willatt, R., Stroeve, J., Tsamados, M., 2023. Synoptic variability in satellite altimeter-derived radar freeboard of Arctic sea ice. Geophysical Research Letters , e2022GL100696doi:10.1029/2022GL100696.

Nandan, V., Geldsetzer, T., Islam, T., Yackel, J.J., Gill, J.P., Fuller, M.C., Gunn, G., Duguay, C., 2016. Ku-, X- and C-band measured and modeled microwave backscatter from a highly saline snow cover on first-year sea ice. Remote Sensing of Environment 187, 62–75. doi:10.1016/J.RSE.2016.10.004.

Nandan, V., Geldsetzer, T., Yackel, J., Mahmud, M., Scharien, R., Howell, S., King, J., Ricker, R., Else, B., 2017a. Effect of Snow Salinity on CryoSat-2 Arctic First-Year Sea Ice Freeboard Measurements. Geophysical Research Letters 44, 419–426. doi:10.1002/2017GL074506.

Nandan, V., Scharien, R., Geldsetzer, T., Mahmud, M., Yackel, J.J., Islam, T., Gill, J.P., Fuller, M.C., Gunn, G., Duguay, C., 2017b. Geophysical and atmospheric controls on Ku-, X- and C-band backscatter evolution from a saline snow cover on first-year sea ice from late-winter to pre-early melt. Remote Sensing of Environment 198, 425–441. doi:10.1016/J.RSE.2017.06.029.

Nandan, V., Scharien, R.K., Geldsetzer, T., Kwok, R., Yackel, J.J., Mahmud, M.S., Rosel, A., Tonboe, R., Granskog, M., Willatt, R., Stroeve, J., Nomura, D., Frey, M., 2020. Snow Property Controls on Modeled Ku-Band Altimeter Estimates of First-Year Sea Ice Thickness: Case Studies from the Canadian and Norwegian Arctic. IEEE Journal of Selected Topics in Applied Earth Observations and Remote Sensing 13, 1082–1096. doi:10.1109/JSTARS.2020.2966432.

Nomura, D., Granskog, M.A., Assmy, P., Simizu, D., Hashida, G., 2013. Arctic and Antarctic sea ice acts as a sink for atmospheric CO2 during periods of snowmelt and surface flooding. Journal of Geophysical Research: Oceans 118. doi:10.1002/2013JC009048.

Nomura, D., Granskog, M.A., Fransson, A., Chierici, M., Silyakova, A., Ohshima, K.I., Cohen, L., Delille, B., Hudson, S.R., Dieckmann, G.S., 2018. CO2 flux over young and snow-covered Arctic pack ice in winter and spring. Biogeosciences 15, 3331–3343. doi:10.5194/BG-15-3331-2018.

Nomura, D., Yoshikawa-Inoue, H., Toyota, T., Shirasawa, K., 2010. Effects of snow, snowmelting and refreezing processes on air–sea-ice CO2 flux. Journal of Glaciology 56, 262–270. doi:10.3189/002214310791968548.

Panzer, B., Gomez-Garcia, D., Leuschen, C., Paden, J., Rodriguez-Morales, F., Patel, A., Markus, T., Holt, B., Gogineni, P., 2013. An ultra-wideband, microwave radar for measuring snow thickness on sea ice and mapping near-surface internal layers in polar firn. Journal of Glaciology 59, 244–254. doi:10.3189/2013JoG12J128.

Panzer, B., Leuschen, C., Patel, A., Markus, T., Gogineni, S., 2010. Ultra-wideband radar measurements of snow thickness over sea Ice. International Geoscience and Remote Sensing Symposium (IGARSS) , 3130–3133doi:10.1109/IGARSS.2010.5654342.

Perovich, D.K., Grenfell, T.C., Light, B., Hobbs, P.V., 2002. Seasonal evolution of the albedo of multiyear Actic sea ice. Journal of Geophysical Research C: Oceans 107. doi:10.1029/2000jc000438.

Perovich, D.K., Grenfell, T.C., Richter-Menge, J.A., Light, B., Tucker, W.B., Eicken, H., 2003. Thin and thinner: Sea ice mass balance measurements during SHEBA. Journal of Geophysical Research: Oceans 108, 8050. doi:10.1029/2001JC001079.

Perovich, D.K., Polashenski, C., 2012. Albedo evolution of seasonal Arctic sea ice. Geophysical Research Letters 39, 8501. doi:10.1029/2012GL051432.

Perovich, D.K., Richter-Menge, J.A., 1994. Surface characteristics of lead ice. Journal of Geophysical Research: Oceans 99, 16341–16350. doi:10.1029/94JC01194.

Petrich, C., Eicken, H., Polashenski, C.M., Sturm, M., Harbeck, J.P., Perovich, D.K., Finnegan, D.C., 2012. Snow dunes: A controlling factor of melt pond distribution on Arctic sea ice. Journal of Geophysical Research: Oceans 117. doi:10.1029/2012JC008192.

Petty, A.A., Keeney, N., Cabaj, A., Kushner, P., Bagnardi, M., 2023. Winter Arctic sea ice thickness from ICESat-2: upgrades to freeboard and snow loading estimates and an assessment of the first three winters of data collection. Cryosphere 17, 127–156. doi:10.5194/TC-17-127-2023.

Petty, A.A., Kurtz, N.T., Kwok, R., Markus, T., Neumann, T.A., 2020. Winter Arctic Sea Ice Thickness From ICESat-2 Freeboards. Journal of Geophysical Research: Oceans 125. doi:10.1029/2019JC015764.

Petty, A.A., Webster, M., Boisvert, L., Markus, T., 2018. The NASA Eulerian Snow on Sea Ice Model (NESOSIM) v1.0: Initial model development and analysis. Geoscientific Model Development 11, 4577–4602. doi:10.5194/gmd-11-4577-2018.

Picard, G., Löwe, H., Domine, F., Arnaud, L., Larue, F., Favier, V., Le Meur, E., Lefebvre, E., Savarino, J., Royer, A., 2022. The Microwave Snow Grain Size: A New Concept to Predict Satellite Observations Over Snow-Covered Regions. AGU Advances 3, e2021AV000630. doi:10.1029/2021AV000630.

Picard, G., Sandells, M., Löwe, H., 2018. SMRT: an active–passive microwave radiative transfer model for snow with multiple microstructure and scattering formulations (v1.0). Geoscientific Model Development 11, 2763–2788. doi:10.5194/gmd-11-2763-2018.

Plante, M., Bailey, D.A., Holland, M.M., DuVivier, A.K., Hunke, E.C., Turner, A.K., 2020. Impact of a New Sea Ice Thermodynamic Formulation in the CESM2 Sea Ice Component. Journal of Advances in Modeling Earth Systems 12. doi:10.1029/2020MS002154.

Polashenski, C., Perovich, D., Courville, Z., 2012. The mechanisms of sea ice melt pond formation and evolution. Journal of Geophysical Research: Oceans 117, 1001. doi:10.1029/2011JC007231.

Popović, P., Finkel, J., Silber, M.C., Abbot, D.S., 2020. Snow Topography on Undeformed Arctic Sea Ice Captured by an Idealized “Snow Dune”

Model. Journal of Geophysical Research: Oceans 125, e2019JC016034. doi:10.1029/2019JC016034.

Pratt, K.A., Custard, K.D., Shepson, P.B., Douglas, T.A., Pöhler, D., General, S., Zielcke, J., Simpson, W.R., Platt, U., Tanner, D.J., Gregory Huey, L., Carlsen, M., Stirm, B.H., 2013. Photochemical production of molecular bromine in Arctic surface snowpacks. Nature Geoscience 2013 6:5 6, 351–356. doi:10.1038/ngeo1779.

Proksch, M., Löwe, H., Schneebeli, M., 2015. Density, specific surface area, and correlation length of snow measured by high-resolution penetrometry. Journal of Geophysical Research: Earth Surface 120, 346–362. doi:10.1002/2014JF003266.

Provost, C., Sennéchael, N., Miguet, J., Itkin, P., Rösel, A., Koenig, Z., Villacieros-Robineau, N., Granskog, M.A., 2017. Observations of flooding and snow-ice formation in a thinner Arctic sea-ice regime during the N-ICE2015 campaign: Influence of basal ice melt and storms. Journal of Geophysical Research: Oceans 122, 7115–7134. doi:10.1002/2016JC012011@10.1002/(ISSN)2169-9291.NICE1.

Pulliainen, J.T., Grandeil, J., 1999. HUT snow emission model and its applicability to snow water equivalent retrieval. IEEE Transactions on Geoscience and Remote Sensing 37, 1378–1390. doi:10.1109/36.763302.

Pulsifer, P., Gearheard, S., Huntington, H.P., Parsons, M.A., McNeave, C., McCann, H.S., 2012. The role of data management in engaging communities in Arctic research: overview of the Exchange for Local Observations and Knowledge of the Arctic (ELOKA). Polar Geography 35, 271–290. doi:10.1080/1088937X.2012.708364.

Riche, F., Schneebeli, M., 2013. Thermal conductivity of snow measured by three independent methods and anisotropy considerations. Cryosphere 7, 217–227. doi:10.5194/TC-7-217-2013.

Ricker, R., Hendricks, S., Perovich, D.K., Helm, V., Gerdes, R., 2015. Impact of snow accumulation on CryoSat-2 range retrievals over Arctic sea ice: An observational approach with buoy data. Geophysical Research Letters 42, 4447–4455. doi:10.1002/2015GL064081.

Riewe, R., 1991. Inuit Use of the Sea Ice. Arctic and Alpine Research 23, 3–10.

Robledano, A., Picard, G., Dumont, M., Flin, F., Arnaud, L., Libois, Q., 2023. Unraveling the optical shape of snow. Nature Communications 2023 14:1 14, 1–11. doi:10.1038/s41467-023-39671-3.

Rostosky, P., Spreen, G., Farrell, S.L., Frost, T., Heygster, G., Melsheimer, C., 2018. Snow Depth Retrieval on Arctic Sea Ice From Passive Microwave Radiometers—Improvements and Extensions to Multiyear Ice Using Lower Frequencies. Journal of Geophysical Research: Oceans 123, 7120–7138. doi:10.1029/2018JC014028.

Royer, A., Roy, A., Montpetit, B., Saint-Jean-Rondeau, O., Picard, G., Brucker, L., Langlois, A., 2017. Comparison of commonly-used microwave radiative transfer models for snow remote sensing. Remote Sensing of Environment 190, 247–259. doi:10.1016/J.RSE.2016.12.020.

Saberi, N., Kelly, R., Flemming, M., Li, Q., 2020. Review of snow water equivalent retrieval methods using spaceborne passive microwave radiometry. International Journal of Remote Sensing 41, 996–1018. doi:10.1080/01431161.2019.1654144.

Savelyev, S.A., Gordon, M., Hanesiak, J., Papakyriakou, T., Taylor, P.A., 2006. Blowing snow studies in the Canadian Arctic Shelf Exchange Study, 2003–04. Hydrological Processes 20, 817–827. doi:10.1002/HYP.6118.

Scharien, R.K., Geldsetzer, T., Barber, D.G., Yackel, J.J., Langlois, A., 2010. Physical, dielectric, and C band microwave scattering properties of first-year sea ice during advanced melt. Journal of Geophysical Research: Oceans 115, 12026. doi:10.1029/2010JC006257.

Scharien, R.K., Segal, R., Nasonova, S., Nandan, V., Howell, S.E., Haas, C., 2017. Winter Sentinel-1 Backscatter as a Predictor of Spring Arctic Sea Ice Melt Pond Fraction. Geophysical Research Letters 44, 262–12. doi:10.1002/2017GL075547.

Schneebeli, M., Johnson, J.B., 1998. A constant-speed penetrometer for high-resolution snow stratigraphy. Annals of Glaciology 26, 107–111. doi:10.3189/1998AOG26-1-107-111.

Schröder, D., Feltham, D.L., Flocco, D., Tsamados, M., 2014. September Arctic sea-ice minimum predicted by spring melt-pond fraction. Nature Climate Change 2014 4:5 4, 353–357. doi:10.1038/nclimate2203.

Schutz, B.E., Zwally, H.J., Shuman, C.A., Hancock, D., DiMarzio, J.P., 2005. Overview of the ICESat Mission. Geophysical Research Letters 32, 1–4. doi:10.1029/2005GL024009.

Segal, R.A., Scharien, R.K., Cafarella, S., Tedstone, A., 2020. Characterizing winter landfast sea-ice surface roughness in the Canadian Arctic Archipelago using Sentinel-1 synthetic aperture radar and the Multi-angle Imaging SpectroRadiometer. Annals of Glaciology 61, 284–298. doi:10.1017/AOG.2020.48.

Shen, X., Ke, C.Q., Li, H., 2022. Snow depth product over Antarctic sea ice from 2002 to 2020 using multisource passive microwave radiometers. Earth System Science Data 14, 619–636. doi:10.5194/ESSD-14-619-2022.

Shi, T., Cui, J., Chen, Y., Zhou, Y., Pu, W., Xu, X., Chen, Q., Zhang, X., Wang, X., 2021. Enhanced light absorption and reduced snow albedo due to internally mixed mineral dust in grains of snow. Atmospheric Chemistry and Physics 21, 6035–6051. doi:10.5194/ACP-21-6035-2021.

Simpson, W.R., Von Glasow, R., Riedel, K., Anderson, P., Ariya, P., Bottenheim, J., Burrows, J., Carpenter, L.J., Frieß, U., Goodsite, M.E., Heard, D., Hutterli, M., Jacobi, H.W., Kaleschke, L., Neff, B., Plane, J., Platt, U., Richter, A., Roscoe, H., Sander, R., Shepson, P., Sodeau, J., Steffen, A., Wagner, T., Wolff, E., 2007. Halogens and their role in polar boundary-layer ozone depletion. Atmospheric Chemistry and Physics 7, 4375–4418. doi:10.5194/ACP-7-4375-2007.

Smith, B.E., Gardner, A., Schneider, A., Flanner, M., 2018. Modeling biases in laser-altimetry measurements caused by scattering of green light in snow. Remote Sensing of Environment 215, 398–410. doi:10.1016/j.rse.2018.06.012.

Smith, M.M., Light, B., Macfarlane, A.R., Perovich, D.K., Holland, M.M., Shupe, M.D., 2022. Sensitivity of the Arctic Sea Ice Cover to the Summer Surface Scattering Layer. Geophysical Research Letters 49, e2022GL098349. doi:10.1029/2022GL098349.

Søgaard, D.H., Kristensen, M., Rysgaard, S., Glud, R.N., Hansen, P.J., Hilligsøe, K.M., 2010. Autotrophic and heterotrophic activity in Arctic first-year sea ice: seasonal study from Malene Bight, SW Greenland. Marine Ecology Progress Series 419, 31–45. doi:10.3354/MEPS08845.

Sommer, C.G., Wever, N., Fierz, C., Lehning, M., 2018. Investigation of a wind-packing event in Queen Maud Land, Antarctica. Cryosphere 12, 2923–2939. doi:10.5194/TC-12-2923-2018.

Sommerfeld, R.A., LaChapelle, E., 1970. The Classification of Snow Metamorphism. Journal of Glaciology 9, 3–18. doi:10.3189/S0022143000026757.

Stirling, I., Andriashek, D., Calvert, W., 1993. Habitat preferences of polar bears in the western Canadian Arctic in late winter and spring. Polar Record 29, 13–24. doi:10.1017/S0032247400023172.

Stirling, I., Smith, T., 2004. Implications of Warm Temperatures and an Unusual Rain Event for the Survival of Ringed Seals on the Coast of Southeastern Baffin Island. Arctic 57, 59–67.

Stroeve, J., Liston, G.E., Buzzard, S., Zhou, L., Mallett, R., Barrett, A., Tschudi, M., Tsamados, M., Itkin, P., Stewart, J.S., 2020a. A Lagrangian Snow-Evolution System for Sea Ice Applications (SnowModel-LG): Part II - Analyses. Journal of Geophysical Research: Oceans 125, e2019JC015900. doi:10.1029/2019JC015900.

Stroeve, J., Nandan, V., Willatt, R., Dadic, R., Rostosky, P., Gallagher, M., Mallett, R., Barrett, A., Hendricks, S., Tonboe, R., Mccrystall, M., Serreze, M., Thielke, L., Spreen, G., Newman, T., Yackel, J., Ricker, R., Tsamados, M., Macfarlane, A., Hannula, H.R., Schneebeli, M., 2022. Rain on snow (ROS) understudied in sea ice remote sensing: a multi-sensor analysis of ROS during MOSAiC (Multidisciplinary drifting Observatory for the Study of Arctic Climate). Cryosphere 16, 4223–4250. doi:10.5194/TC-16-4223-2022.

Stroeve, J., Nandan, V., Willatt, R., Tonboe, R., Hendricks, S., Ricker, R., Mead, J., Mallett, R., Huntemann, M., Itkin, P., Schneebeli, M., Krampe, D., Spreen, G., Wilkinson, J., Matero, I., Hoppmann, M., Tsamados, M., 2020b. Surface-based Ku- and Ka-band polarimetric radar for sea ice studies. The Cryosphere 14, 4405–4426. doi:10.5194/tc-14-4405-2020.

Stroeve, J., Serreze, M.C., Holland, M.M., Kay, J.E., Malanik, J., Barrett, A.P., 2012. The Arctic's rapidly shrinking sea ice cover: A research synthesis. Climatic Change 110, 1005–1027. doi:10.1007/s10584-011-0101-1.

Stroeve, J., Vancoppenolle, M., Veyssiere, G., Lebrun, M., Castellani, G., Babin, M., Karcher, M., Landy, J., Liston, G.E., Wilkinson, J., 2021. A Multi-Sensor and Modeling Approach for Mapping Light Under Sea Ice During the Ice-Growth Season. Frontiers in Marine Science 7, 1253. doi:10.3389/fmars.2020.592337.

Sturm, M., 1989. The role of thermal convection in heat and mass transport in the subarctic snow cover. Ph.D. thesis. University of Alaska Fairbanks.

Sturm, M., Holmgren, J., 2018. An Automatic Snow Depth Probe for Field Validation Campaigns. Water Resources Research 54, 9695–9701. doi:10.1029/2018WR023559.

Sturm, M., Holmgren, J., Perovich, D.K., 2002. Winter snow cover on the sea ice of the Arctic Ocean at the Surface Heat Budget of the Arctic Ocean (SHEBA): Temporal evolution and spatial variability. Journal of Geophysical Research C: Oceans 107, 1–17. doi:10.1029/2000jc000400.

Sturm, M., Massom, R.A., 2016. Snow in the sea ice system: Friend or foe? Sea Ice: Third Edition , 65–109doi:10.1002/9781118778371.ch3.

Sturm, M., Morris, K., Massom, R., 1998. The Winter Snow Cover of the West Antarctic Pack Ice: Its Spatial and Temporal Variability. Antarctic sea ice: physical processes, interactions and variability 74, 1–18. doi:10.1029/AR074P0001.

Szabo, D., Schneebeli, M., 2007. Subsecond sintering of ice. Applied Physics Letters 90. doi:10.1063/1.2721391/166975.

Thielke, L., Fuchs, N., Spreen, G., Tremblay, B., Birnbaum, G., Huntemann, M., Hutter, N., Itkin, P., Jutila, A., Webster, M.A., 2023. Preconditioning of Summer Melt Ponds From Winter Sea Ice Surface Temperature. Geophysical Research Letters 50, e2022GL101493. doi:10.1029/2022GL101493.

Tian, L., Gao, Y., Weissling, B., Ackley, S.F., 2020. Snow-ice contribution to the structure of sea ice in the Amundsen Sea, Antarctica. Annals of Glaciology 61, 369–378. doi:10.1017/AOG.2020.55.

Tian, T., Yang, S., Høyer, J.L., Nielsen-Englyst, P., Singha, S., 2024. Cooler Arctic surface temperatures simulated by climate models are closer to satellite-based data than the ERA5 reanalysis. Communications Earth & Environment 2024 5:1 5, 1–6. doi:10.1038/s43247-024-01276-z.

Tilling, R.L., Ridout, A., Shepherd, A., 2018. Estimating Arctic sea ice thickness and volume using CryoSat-2 radar altimeter data. Advances in Space Research 62, 1203–1225. doi:10.1016/j.asr.2017.10.051.

Tison, J.L., Delille, B., Papadimitriou, S., 2016. Gases in sea ice. Sea Ice: Third Edition , 433–471doi:10.1002/9781118778371.CH18.

Tjuatja, S., Fung, A.K., Bredow, J., 1992. Scattering Model for Snow-Covered Sea Ice. IEEE Transactions on Geoscience and Remote Sensing 30, 804–810. doi:10.1109/36.158876.

Trujillo, E., Leonard, K., Maksym, T., Lehning, M., 2016. Changes in snow distribution and surface topography following a snowstorm on Antarctic sea ice. Journal of Geophysical Research: Earth Surface 121, 2172–2191. doi:10.1002/2016JF003893.

Tsang, L., Chen, C.T., Chang, A.T., Guo, J., Ding, K.H., 2000. Dense media radiative transfer theory based on quasicrystalline approximation with applications to passive microwave remote sensing of snow. Radio Science 35, 731–749. doi:10.1029/1999RS002270.

Tucker, W.B., Perovich, D.K., Gow, A.J., Weeks, W.F., Drinkwater, M.R., 2011. Physical properties of sea ice relevant to remote sensing, in: Microwave Remote Sensing of Sea Ice. 1 ed.. American Geophysical Union (AGU), pp. 9–28. doi:10.1029/gm068p0009.

Vérin, G., Domine, F., Babin, M., Picard, G., Arnaud, L., 2022. Metamorphism of Arctic marine snow during the melt season. Impact on spectral albedo and radiative fluxes through snow. The Cryosphere Discussions 2022, 1–27. doi:10.5194/tc-2022-76.

Veyssière, G., Castellani, G., Wilkinson, J., Karcher, M., Hayward, A., Stroeve, J.C., Nicolaus, M., Kim, J.H., Yang, E.J., Valcic, L., Kauker, F., Khan, A.L., Rogers, I., Jung, J., 2022. Under-Ice Light Field in the Western Arctic Ocean During Late Summer. Frontiers in Earth Science 9, 643737. doi:10.3389/FEART.2021.643737/BIBTEX.

Vionnet, V., Brun, E., Morin, S., Boone, A., Faroux, S., Le Moigne, P., Martin, E., Willemet, J.M., 2012. The detailed snowpack scheme Crocus and its implementation in SURFEX v7.2. Geoscientific Model Development 5, 773–791. doi:10.5194/gmd-5-773-2012.

Wang, J., Gough, W.A., Yan, J., Lu, Z., 2022. Ecological Risk Assessment of Trace Metal in Pacific Sector of Arctic Ocean and Bering Strait Surface Sediments. International Journal of Environmental Research and Public Health 2022, Vol. 19, Page 4454 19, 4454. doi:10.3390/IJERPH19084454.

Warren, S.G., Rigor, I.G., Untersteiner, N., Radionov, V.F., Bryazgin, N.N., Aleksandrov, Y.I., Colony, R., 1999. Snow depth on Arctic sea ice. Journal of Climate 12, 1814–1829. doi:10.1175/1520-0442(1999)012<1814:SDOASI>2.0.CO;2.

Webster, M., Gerland, S., Holland, M., Hunke, E., Kwok, R., Lecomte, O., Massom, R., Perovich, D., Sturm, M., 2018. Snow in the changing sea-ice systems. Nature Climate Change 8, 946–953. doi:10.1038/s41558-018-0286-7.

Webster, M.A., DuVivier, A.K., Holland, M.M., Bailey, D.A., 2021. Snow on Arctic Sea Ice in a Warming Climate as Simulated in CESM. Journal of Geophysical Research: Oceans 126, e2020JC016308. doi:10.1029/2020JC016308.

Webster, M.A., Holland, M., Wright, N.C., Hendricks, S., Hutter, N., Itkin, P., Light, B., Linhardt, F., Perovich, D.K., Raphael, I.A., Smith, M.M., Von Albedyll, L., Zhang, J., 2022. Spatiotemporal evolution of melt ponds on Arctic sea ice: MOSAiC observations and model results. Elementa 10. doi:10.1525/ELEMENTA.2021.000072/169460.

Webster, M.A., Parker, C., Boisvert, L., Kwok, R., 2019. The role of cyclone activity in snow accumulation on Arctic sea ice. Nature Communications 2019 10:1 10, 1–12. doi:10.1038/s41467-019-13299-8.

Webster, M.A., Rigor, I.G., Nghiem, S.V., Kurtz, N.T., Farrell, S.L., Perovich, D.K., Sturm, M., Webster, M.A., Rigor, I.G., Nghiem, S.V., Kurtz, N.T., Farrell, S.L., Perovich, D.K., Sturm, M., 2014. Interdecadal changes in snow depth on Arctic sea ice. Journal of Geophysical Research : Oceans 119, 5395–5406. doi:10.1002/2014JC009985.Received.

Webster, M.A., Rigor, I.G., Perovich, D.K., Richter-Menge, J.A., Polashenski, C.M., Light, B., 2015. Seasonal evolution of melt ponds on Arctic sea ice. Journal of Geophysical Research: Oceans 120, 5968–5982. doi:10.1002/2015JC011030.

Wever, N., Rossmann, L., Maaß, N., Leonard, K.C., Kaleschke, L., Nicolaus, M., Lehning, M., 2020. Version 1 of a sea ice module for the physics-based, detailed, multi-layer SNOWPACK model. Geoscientific Model Development 13, 99–119. doi:10.5194/gmd-13-99-2020.

Wiesmann, A., Fierz, C., Mätzler, C., 2000. Simulation of microwave emission from physically modeled snowpacks. Annals of Glaciology 31, 397–401. doi:10.3189/172756400781820453.

Willatt, R., Laxon, S., Giles, K., Cullen, R., Haas, C., Helm, V., 2011. Ku-band radar penetration into snow cover on Arctic sea ice using airborne data. Annals of Glaciology 52, 197–205. doi:10.3189/172756411795931589.

Willatt, R., Stroeve, J.C., Nandan, V., Newman, T., Mallett, R., Hendricks, S., Ricker, R., Mead, J., Itkin, P., Tonboe, R., Wagner, D.N., Spreen, G., Liston, G., Schneebeli, M., Krampe, D., Tsamados, M., Demir, O., Wilkinson, J., Jaggi, M., Zhou, L., Huntemann, M., Raphael, I.A., Jutila, A., Oggier, M., 2023. Retrieval of Snow Depth on Arctic Sea Ice From Surface-Based, Polarimetric, Dual-Frequency Radar Altimetry. Geophysical Research Letters 50, e2023GL104461. doi:10.1029/2023GL104461.

Willatt, R.C., Giles, K.A., Laxon, S.W., Stone-Drake, L., Worby, A.P., 2010. Field investigations of Ku-band radar penetration into snow cover on antarctic sea ice. IEEE Transactions on Geoscience and Remote Sensing 48, 365–372. doi:10.1109/TGRS.2009.2028237.

WMO, 2022. The 2022 GCOS Implementation Plan. Technical Report. World Meteorological Organisation.

Wongpan, P., Nomura, D., Toyota, T., Tanikawa, T., Meiners, K.M., Ishino, T., Tamura, T.P., Tozawa, M., Nosaka, Y., Hirawake, T., Ooki, A., Aoki, S., 2020. Using under-ice hyperspectral transmittance to determine land-fast sea-ice algal biomass in Saroma-ko Lagoon, Hokkaido, Japan. Annals of Glaciology 61, 454–463. doi:10.1017/AOG.2020.69.

Worby, A.P., Geiger, C.A., Paget, M.J., Van Woert, M.L., Ackley, S.F., DeLiberty, T.L., 2008. Thickness distribution of Antarctic sea ice. Journal of Geophysical Research: Oceans 113, 5–92. doi:10.1029/2007JC004254.

Yackel, J., Geldsetzer, T., Mahmud, M., Nandan, V., Howell, S.E., Scharien, R.K., Lam, H.M., 2019. Snow thickness estimation on first-year sea ice from late winter spaceborne scatterometer backscatter variance. Remote Sensing 11. doi:10.3390/rs11040417.

Yackel, J.J., Barber, D.G., Hanesiak, J.M., 2000. Melt ponds on sea ice in the Canadian Archipelago: 1. Variability in morphological and radiative properties. Journal of Geophysical Research: Oceans 105, 22049–22060. doi:10.1029/2000JC900075.

Yang, X., Pyle, J.A., Cox, R.A., 2008. Sea salt aerosol production and bromine release: Role of snow on sea ice. Geophysical Research Letters 35. doi:10.1029/2008GL034536.